Het verkeerskundig
laboratorium
voor studenten

ITS EDU LAB

Energy efficient electric vehicle platooning at signalized intersections

R.K.Muniyandi
4791495

Rijkswaterstaat
Ministry of Infrastructure and Water Management

TU Delft

Colophon

In partial fulfilment of the requirements for the degree of **Master of Science** in Mechanical Engineering at the Delft University of Technology, to be defended publicly on Wednesday December 16th, 2020 at 10:00 a.m.

Author

R.K.Muniyandi
Delft University of Technology
Faculty of Mechanical, Maritime and Materials Engineering (3mE)
Master student Vehicle Engineering

Graduation Committee

Dr. ir. Riender Happee
Examination chair
Associate Professor
TU Delft, CiTG, Transport & Planning

Dr. ir. Meng Wang
Daily supervisor
Assistant Professor
TU Delft, CiTG, Transport & Planning

Mr. ir. Marco Schreuder
External supervisor
Senior Advisor and Coordinator Active Traffic Management
Rijkswaterstaat

Dr. Laura Ferranti
Assistant Professor
Cognitive Robotics (CoR) Department,
TU Delft, 3ME

Published by ITS Edulab, Delft

Date December 5, 2020

Status Final report

ITS Edulab is a cooperation between Rijkswaterstaat and Delft University of Technology

TU Delft

Rijkswaterstaat
Ministry of Infrastructure and Water Management

Acknowledgement

எந்நன்றி கொன்றார்க்கும் உய்வுண்டாம் உய்வில்லை
செய்ந்நன்றி கொன்ற மகற்கு.
- திருவள்ளுவர்

First and foremost I would like to thank my supervisor and guide **Dr. ir. Meng Wang**, for giving me the opportunity to work on a topic of interest to me. Meng was always available to listen to my ideas, discuss concepts and clarify the fundamental doubts. Meng also patiently reviewed several revisions of the thesis, pointing out minute things that could make it better, for which I am very grateful. I am also thankful to **Dr. ir. Riender Hapee** for his insights on the research and consenting to be my supervisor and chair from the Department of Mechanical Engineering. My special thanks to **Mr. ir. Marco Schreuder**, my supervisor at Rijkswaterstaat and **Mr. Ronald Adams**, for providing me with the industrial insights and opportunity to travel to China for my research.

My gratitude goes out to the team at RIOH (Research Institute of Highways, China), **Mr. Gao Jian**, **Dr. Huang** and **Mr. Yiding Li** for their valuable suggestions and hospitality. I would also like to thank my friend **Zixiao Liu** for helping me with almost everything, from language to navigation during my stay in China. I would cherish our times at the library in Beijing university of technology. I also thank **Daan** and **Renee** for working alongside with me in Rijkswaterstaat.

My special thanks to **Kunal**, **Yash** and **Siddharth** for the many valuable discussions on technical concepts and for helping out with the questions I had. I would like to thank my few but close friends in the Netherlands: **Vasu**, **Keerthana**, **Ram**, **Madhan**, **Siddharth**, **Subhi**, **Pragati** and **Sibi**. They made my Masters journey much easier and memorable. All the video calls and online games with them were especially invaluable during the Covid lockdown. I would also like to thank my housemate and friend, **Jishnu** for all the good times and movie nights with Vasu and Madhu.

To my best friends from India, **Jose**, **Akhil**, **Lux**, **Swathi** and **Rash**, thank you for cheering me up during my difficult times. To the person who has been a pillar of support and encouragement: **Madhu**, I cannot emphasize, how grateful I am. You made this entire journey very easy.

Last but not the least, my heartfelt gratitude to my family, who have always been my biggest supporters. This thesis is dedicated to my sister: **Vinodhini**, who is my inspiration, and my parents: **Muniyandi** and **Poongodi**, whose belief, unconditional love and support has made me what I am today. I am eternally indebted to them.

Raj Kumar Muniyandi
Delft, December 2020

Abstract

Growth of mobility for people and goods transportation has been increasing steadily over the years. With the perpetual increase in number of road vehicles, comes the inevitable problems of traffic and pollution. Various intelligent traffic technologies and strategies have been proposed and implemented over the years to overcome the road traffic problems. Platooning is identified as one of the ways to tackle transportation related problems efficiently. Even though platooning has been tested and implemented in highways, not much attention has been given to controlling the platoons at urban roads. When vehicles in the platoon are connected and automated, it helps them to understand the environment better and communicate efficiently for better performance. Platoons at the vicinity of signalized intersections need to accelerate and decelerate in a nonlinear manner which leads to higher energy consumption and longer travel time. Most of the previous research approaches focused on optimizing only the energy consumption or travel time of the platoons. However, studies show that the recommended driving advice from the controllers is not tracked by the drivers completely.

The current research focuses on optimal trajectory planning of the electric vehicle platoons at signalized intersections. This is done by designing an energy efficient longitudinal controller for the platoons using optimal control method. The goal of this thesis is split between planning and tracking the trajectory. Thus the optimal speed profile is planned by the high level controller (i.e the optimal controller) and tracked using a battery electric vehicle model controlled by a low level controller (i.e a PID controller). The performance of the controlled platoon was verified using different scenarios and was found to perform positively under respective control objectives and constraints. The designed controlled and automated platoon by the optimal controller was able to achieve energy consumption and cost saving up to 67% when compared with intelligent driver model (IDM) platoon for a specific scenario.

This research is a collaboration between the **Research Institute of Highways (RIOH)** in China and **Rijkswaterstaat, Ministry of Infrastructure and Water Management** in The Netherlands, to overcome the common traffic problems on road. The research was carried out at the **ITS-Edulab**, a Dutch traffic and transport laboratory for students. It is a cooperation between **Rijkswaterstaat** and the Transport & Planning group of the **Delft University of Technology**.

Keywords: platooning, electric vehicles, energy consumption, nonlinear optimization, optimal control.

Contents

List of figures and tables

List of Figures

List of Tables

1. Introduction

Traffic congestion growth has been consistent all over the world both in developed and underdeveloped countries. The rapid growth also indicates that it will get even worse and prove to be a hazard to the quality of urban life. Its prominent effect is continuous reduction in traffic speeds, resulting in increased travel times, fuel/energy consumption, driver stress and environmental pollution [1]. In particular, the freight traffic in EU is expected to double within the next 15 years [2]. This made the scientists and researchers in Intelligent Transport Systems (ITS) to look for various solutions to increase the performance of the existing traffic and transportation systems. One such technology for addressing this issue is platooning. Platooning of vehicles has advantages such as: increasing traffic capacity, reducing fuel consumption and decreasing the driver's stress while driving in urban conditions. Even though platooning has lot of positive effects with the traffic environment, it has some drawbacks which has to be addressed to make platooning viable solution in day-to-day life. This research is a step in the direction to efficiently implement platooning at intersections in urban areas.

1.1. Background

1.1.1. Vehicle platooning

A platoon is a group of vehicles following each other at small distances or headway between them. Platooning is a convoy of vehicles following each other at a very small headway either semi-autonomously or fully autonomously with the help of automated driving technology. This technology benefits the transportation company by reducing the fuel consumption and increasing the productivity of the driver [3]. In platooning, the vehicles are generally controlled longitudinally by adjusting the headway between them by acceleration or deceleration. When vehicles drive in each other's slipstream, it results in increasing the efficiency of traffic flow, reducing the fuel consumption of vehicles and CO_2 emissions to a greater extent. Platooning also helps in optimizing the road usage, since the area occupied by the platoon is lesser than the area occupied by the individual vehicles. The vehicle at the head of the platoon acts as the leader, with the follower vehicles reacting and adapting to the changes in the leader's movement using little or no action from the drivers. Normally, the drivers are in control at all times so that they can decide to let the platoon operate on its own when required and take back control during emergencies.

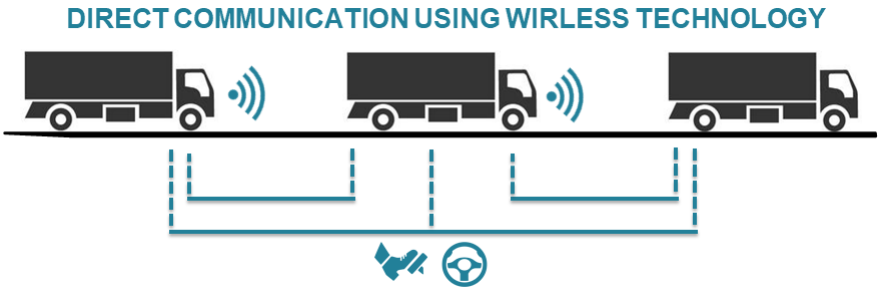

Figure 1.1. – Truck platooning illustration

Platooning can be performed with the help of Adaptive Cruise Control (ACC) and Co-operative Adaptive Cruise Control (CACC). Further CACC systems can be improved with the help of Vehicle to Vehicle (V2V) and/or Vehicle to Infrastructure (V2I) communication. Using various communication systems the follower vehicles maintain a very small headway between the leader vehicle without rear-end crashes [4]. Platooning has the potential to make road transport safer, cleaner, and more efficient if implemented on highways. When the vehicles drive close to each other, the air-drag friction is reduced significantly. Peleton technology has reported an overall 7% fuel saving from platooning (4% for the lead truck and 10% for the following trucks). The intelligent driving technology in platooning systems helps in tight formation which reacts quickly to emergencies through automatic braking. The follower vehicles only need one-fifth of the time a human would need to react and thus helping to improve the overall safety of the journey.

1.1.2. Eco driving

Eco-driving is a very viable option to reduce traffic and fuel consumption of vehicles in the transportation sector. It provides real-time driving advice to the drivers, which when followed results in increased fuel efficiency. Eco driving can be applied to almost every powertrain types. In electric vehicles, the driving behavior significantly influences the energy consumption of the EV. This can be changed by eco-driving maneuvers as it helps in increasing the range of the battery by optimizing the energy consumption. Numerous studies have indicated that eco-driving can reduce fuel consumption by 17 % on average [5].

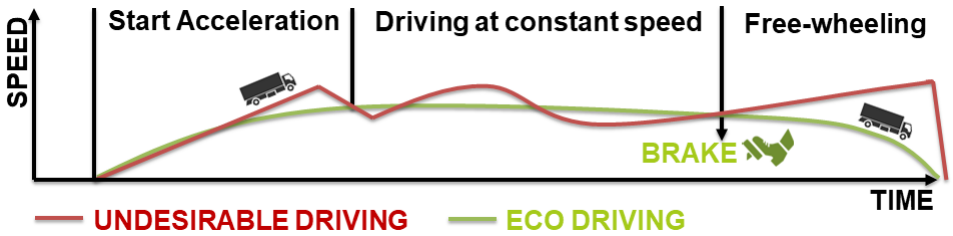

Figure 1.2. – Eco driving illustration

Frequent accelerations associated with the stop and go waves are followed by excessive

speeds, slow movements, and long idling time during congestion. These are the major factors for the increase in fuel/energy consumption [6]. Eco-driving approaches are commonly categorized into freeway based and arterial based strategies. In freeways, the vehicles are not affected by traffic signals and the traffic stream is almost continuous. For freeways, the eco-driving strategies are usually based on computing advisory speed or speed limits for the drivers with the help of V2I or V2V communication. But in arterial roads, there are traffic signals which are used to control the stream of vehicles. The vehicles are stopped ahead of traffic signal during red indications which results in shock waves within the stream. Thus the vehicles are made to accelerate/decelerate and also stay idle which increases the fuel consumption of vehicles. Eco-driving strategies can be designed in such a way to reduce the idle time during a red light in traffic and hard acceleration by advising the drivers to approach the intersections using a modified acceleration and deceleration strategy [7]. Connected vehicles (CVs) are also developed which enabled individual vehicles to reduce fuel consumption. CV technology enables vehicles to interact with road traffic information and communicate with traffic controllers to receive signal phase and timing (SPaT) which is used to calculate fuel optimized trajectories for arterial roads [8]. Applications like Eco Approach and Departure (EAD) also included velocity planning algorithm for maximizing the probability of approaching the junction during green light using the traffic signal information. Further, the EAD system was improved by including the surrounding traffic information to create energy-efficient vehicle speed profiles [5].

1.1.3. Predictive cruise control

Cruise control has now become a standard system in most of the cars and trucks for aiding the driver and helping in maintaining fuel efficiency on long flat routes. Adaptive cruise control (ACC) will help in saving fuel in higher traffic scenarios by maintaining a safe following distance from the preceding vehicle. But when the topology of the road changes such as inclination or grade, the fuel consumption needed to maintain a constant speed is high. Therefore, conventional cruise control and ACC systems fail during sudden changes in road topology. Predictive cruise control (PCC) helps to overcome this drawback by using the information of the vehicle's environment to adjust the vehicle speed. If the vehicle approaches an incline, the PCC helps to increase the speed of the vehicle before it reaches the incline so that the vehicle need not waste a lot of fuel/energy in ascending the incline. PCC uses GPS technology to establish the precise location of the vehicle and to know the necessary driving conditions that have to be taken into account over the next look ahead distance. *Erik Hellstrom* [9] reported that the PCC can be used to minimize the fuel consumption and trip time by using it as a look ahead controller. It showed a 3.5% fuel reduction on a 120km route without an increase in trip time. The paper used a dynamic programming and real-time experiments to validate the approach. *Lattemann* [10] used simulations with 3D road models to validate the PCC, which showed up to a 4.05% reduction in fuel consumption when compared with conventional cruise control systems.

Over the years, PCC was also used for improving the fuel economy and travel time using the upcoming traffic signal information. *Asadi and Vahidi* [11] proposed an optimization-based algorithm that uses short-range radar and traffic signal information predictively to calculate the optimum velocity trajectory for the vehicle. The algorithm was used in various

trail runs and it was found that predictive use of signal timing reduced the fuel consumption by 47%. Most of the literature on PCC do not discuss the characteristics of hybrid electric vehicles (HEV) or electric vehicles (EV). Therefore, a combination of optimal velocity trajectory construction and ACC is presented as PCC for HEV by *T Van Keulen* [12].

1.1.4. Green light optimal speed advisory

The need for reducing energy consumption and travel time during the traffic signals accounted for the introduction of green light optimal speed advisory (GLOSA) systems. The GLOSA takes advantage of I2V communication to optimize traffic efficiency. GLOSA uses accurate information about traffic signal timings and traffic signal locations, to advise the drivers to maintain or choose the speed for a more uniform driving pattern with less stopping time through traffic signals [13]. The future states or information of the signal timings are very critical for GLOSA. Many vehicles will receive GLOSA to arrive at the same green phase, this also leads to platoon formation. The advised speed is calculated by various methods that are characterized by the objective function which contains factors such as fuel consumption and travel time. Road and traffic data along with traffic signal and phase timing are also used by advisory algorithms to calculate the traffic light schedules with higher accuracy. *Sanchez et al.* inspected the effect of a GLOSA-like algorithm on fuel consumption in an I2V environment. It was found that if just one out of 10 vehicles were equipped with GLOSA, it resulted in about 30% reduction in fuel consumption of all vehicles [14]. *Katsaros et al.* tested GLOSA-like scenario for a two-intersection model developed in SUMO, the research showed that increasing the penetration rate of GLOSA equipped vehicles results in reduced fuel consumption and traffic congestion [15].

From the previous works, it is evident that slow and go driving pattern is better than stop and go driving pattern. It was found that about 20 percent more fuel will be used when vehicles accelerate from a full stop to eight kilometers per hour. GLOSA approaches are classified into two types, single and multi-segment. In single segment approaches the advisory speed is only calculated for the next immediate segment to the nearest traffic signal.

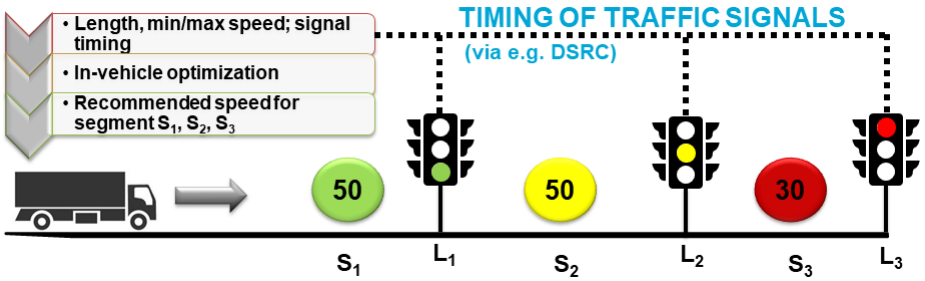

Figure 1.3. – GLOSA: Multi-segment approach: calculation of optimal speeds for forth coming segments

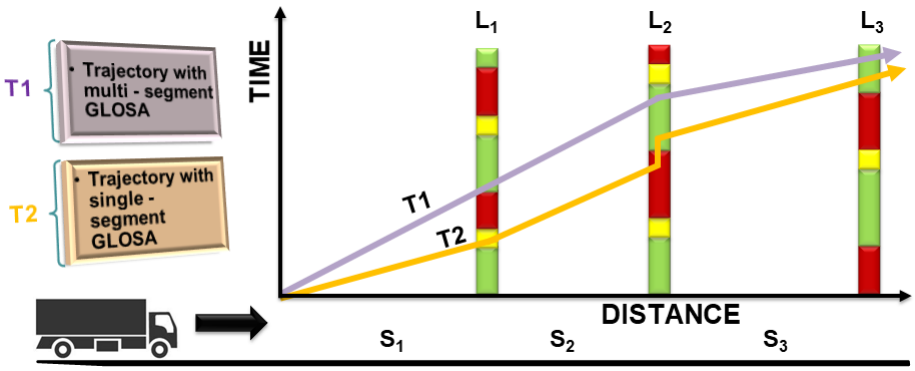

Figure 1.4. – GLOSA: Time-space diagram of trajectories for single and multi segment approaches

In multi-segment GLOSA, a vehicle calculates a set of optimal speeds for the forthcoming segments before entering the first segment as shown in figure 1.3. The trajectories of vehicles for single and multi-segment GLOSA at signalized intersections are shown in figure 1.4 as T1 and T2. It can be seen that the travel time for both the approaches are closely similar. But the trajectory of single-segment T1 is less efficient, as it has to stop at the red light at segment s_2. But since the T2 uses multi-segment GLOSA, the vehicle gets optimal advisory speeds such that it can pass through green phases at all segments. Thus reducing the travel time and increasing the fuel efficiency of the vehicle [16].

1.2. Problem definition

While technologies like PCC, GLOSA, and Eco-driving helped in advising the driver with optimal speed for efficient driving, the advised speed could not be matched by the driver efficiently. Later, the era of automation and connected vehicle technologies took advantage of the intelligence of the vehicles to overcome the challenges of increased travel time and energy consumption of vehicles in traffic intersections, making automation in urban traffic scenario still an area for research. Intersections have a major influence on traffic. They are the primary traffic bottleneck of traffic flow, travel time, pollution, and fuel efficiency. At signalized intersections, vehicles have to stop during the red phase. Thus this research will focus on electric truck platooning at intersections and also the design of an energy-efficient longitudinal controller with minimized travel time.

1.3. Research objective

The main objective of the research is to design an energy efficient longitudinal controller for electric vehicle platoons at signalized intersections which is capable of minimizing the travel delay and energy consumption rate simultaneously.

1.4. Research scope

The research scope explains the extent to which the research area will be explored in this work and specifies the focus of the research. The scope of this research is bounded by various ways as follows:

- The platoon is only controlled longitudinally.
- The vehicles are considered to already be in a platoon.
- All the vehicles in the platoon are considered to have the same dynamics and characteristics.
- All the vehicles in the platoon are considered to be Battery Electric Vehicles (BEVs).
- The vehicle model used in this research for tracking the optimal speed profile from the controller is considered to be a standalone system (i.e) There is no feedback from the vehicle model to the optimal controller.
- The designed controller is only tested through simulations.

1.5. Report outline

This thesis report is divided into five parts that correspond to the five phases of the research. Chapter 2 discusses the literature study, consisting of three parts: research on the existing longitudinal control strategies for truck platoons at signalized intersections, research on the state-of-the-art of energy consumption models for calculating instantaneous energy consumption rate and the knowledge gaps in the existing literature. Chapter 3 concerns design of the optimal controller for longitudinal control of the platoons at signalized intersections and modelling of energy consumption models. Chapter 4 explains about the longitudinal electric vehicle model modelled in Simulink for tracking the optimal speed profile from the controller. Next, Chapter 5 discusses the testing scenarios and the simulation results. Finally, conclusions are drawn, the limitations of the research are addressed, a reflection given and recommendations are made in Chapter 6.

2. Literature review

In this chapter a literature study is carried out to design an optimal control algorithm for electric vehicle platoons in signalized intersections. The literature study helps in understanding the state-of-the-art control algorithms in the area of research. It also aims to identify the knowledge gaps on platooning at intersections. Since this thesis mainly focuses on electric vehicle platoons, modelling instantaneous energy consumption rate is considered to be very vital.
In section 2.1, an overview of the existing state-of-the-art longitudinal control strategies are explored on the basis of eco-driving methods for driving at signalized intersections. In Section 2.2, different state-of-the-art energy consumption models are discussed. The factors influencing the energy consumption models are also explained. Finally, the limitations and gaps in the existing literature are addressed.

2.1. Overview of longitudinal control strategies at the intersection

Over the years a lot of work has been done on vehicle platooning. There have been various models and algorithms developed for making platooning a reality. Even though platooning at highways is a well-proven concept, it has to overcome a lot of challenges in urban areas filled with lot of signals. At signalized intersections, the vehicles have to stop at the red light phase and start again during the green light phase. The behavior of the vehicles is affected by the intersections as they have to accelerate, decelerate, or even stop. This causes increased fuel consumption, emission, travel delay, and even traffic shortwaves. To minimize these effects, most of the research has been carried out on the traffic signal control algorithms to make them more adaptive and dynamic for the traffic scenario. However, with the era of intelligent vehicle technologies, it is time to switch the focus on control strategies on vehicles to overcome the problems. Knowledge of the traffic lights signal timings has been significantly beneficial in terms of energy efficiency in urban traffic. Developments like GLOSA has shown promising advantages in terms of fuel consumption and average idling time.

Many algorithms and methods have been developed for the reduction of fuel consumption and emissions in the automobile sector. Researchers have proposed several eco-driving methods that can be used for optimizing EV energy efficiency under driving conditions. An ecofriendly energy optimal adaptive cruise (ACC) was developed [17]. It calculates an energy optimal trajectory while following another slower vehicle in traffic. A fuzzy logic system was used to calculate the energy efficiency and eco-score which was informed to the driver with the help of an android application [18]. Mechanical systems were also modified to overcome the problem of fuel consumption by introducing a torque vectoring control system [19]. It can optimally distribute the torque by considering the efficiency attributes of EVs and was identified to be improving the energy-efficient by 10%.

Most of the recent research is focused on developing connected vehicles (CVs) and connected and automated vehicle (CAVs) technologies to improve the sustainability of transportation. These technologies enable control of individual vehicles to minimize fuel consumption levels. CV technologies enable vehicles to exchange road traffic information and to communicate with road traffic signal controllers to receive information on signal phase and timings (SPaT). This information can be used to estimate the fuel-efficient trajectories for vehicles at intersections. Programs such as the eCoMove and Compass4D were initiated by the European Union in which the traffic information can be shared with the road users and infrastructure in real-time to enable more efficient and sustainable transportation. The AERIS (Application for the Environment: Real Tine Information Synthesis) initiated by the U.S. Department of Transportation is a collective group of CV applications that were specifically designed for eco-friendly transportation [20]. Also, CAV technology can be driven by itself with the help of on-board perception sensors, and also communicate with the driver, roadside vehicles, infrastructure, and the cloud [21].

CAV technology also produces significant mobility and safety benefits. The cooperative adaptive cruise control (CACC) enables the CAVs to cooperate to form vehicle strings. Eco-driving is also integrated with CACC systems for traffic at signalized intersections. Yang *et al* in [22] developed an Eco-CACC algorithm for an isolated signalized intersection, which computes the fuel-optimum trajectory to make sure that the CAV reaches the traffic intersections as soon as the last CAV in the queue has passed the intersections. Nearly all these researches assist the drivers in their travel along the signalized intersections by providing fuel optimum trajectories. These are often categorized as eco-driving at signalized intersections and are known with specific names like GLOSA (Green Light Optimised Speed Advisory) or Eco-Approach and Departure (EAD). The Eco-approach and Departure are one of the CV applications under the AERIS program. The EAD has been identified as a promising approach in terms of reducing fuel consumption and emissions. Like the other eco-driving techniques at intersections, EAD utilizes the signal phase and timing (SPaT) information from the upcoming traffic to compute a fuel optimum speed profile that minimizes vehicle energy consumption and emissions when approaching and departing the intersection. The estimated speed profile is conveyed to the driver with the help of driver-vehicle interfaces (DVI's).

The EAD application was further developed by integrating the vehicle trajectory planning algorithm (VTPA) with model predictive control (MPC) to develop a partially automated EAD system for EVs as in [23]. In this work, the control objective is to follow the recalculated optimal trajectory as close as possible for each optimization time horizon. The queue effect at signalized intersections is considered while planning the fuel-efficient velocity profile in [24]. Xia *et al* [25] and Hao *et al* [26] improved the EAD system with the consideration of surrounding traffic to estimate vehicle speed profiles. But in these studies, the queue length is assumed to detect with the help of onboard sensors which is not realistic, as the queue length ahead of intersection changes over time. The penetration rate of connected vehicles also plays a major role.

Cooperative vehicles consist of great potential to enhance traffic efficiency and fuel economy on urban roads with signalized intersections. Many optimal control approaches have

been developed so far to optimize the trajectories of cooperative vehicles at fixed timing signalized intersections along the arterial. Even though a lot of research has been done over the years on cooperative vehicle platooning on highways, less attention has been given to the design of CAV platoons at urban roads. The research on trajectory optimization of CAV systems can be grouped into two categories: vehicle to vehicle-based (V2V) trajectory control and vehicle to infrastructure (V2I) based speed advice/control. The V2V trajectory control methods uses reliable communication between vehicles to improve traffic efficiency and avoid a collision which further reduces travel time and delay. But most of these algorithms were confined to isolated intersections without other road users which were not realistic. As for V2I based algorithms, they were usually speeding advice systems which guide the driver or the vehicle to pass the intersection in an energy-efficient manner.

The GLOSA system was designed to help drivers with speed advice on urban corridors by calculating travel time to the stop line. These systems were identified to optimize fuel consumption and travel delays. It is usually implemented as an optimization model by assuming a simple speed pattern in front of the intersection [27]. [28] considered a fuel consumption model in the objective function and showed that simplified objective functions like minimizing the deceleration or idling time would not result in the optimization of fuel consumption. The research was further extended to control the variable speed limit for each vehicle to minimize fuel consumption [29]. Yang *et al* added queue estimation to the same research [30]. The impact of different trajectories on fuel consumption was analyzed in [31] in which the vehicles were advised to use small deceleration, combined with a period of constant speed in place of hard decelerations in front of red light. Stebbins *et al* devised a method that suggests an acceleration to the platoon leader to reduce the delays. It was assumed that every vehicle that is the first to pass the intersection on green light can be selected as a leading vehicle [27]. A green driving strategy to control the individual advisory speed limit of the connected vehicles while following their leaders at signalized intersections was also proposed. The strategy can be applied to any level of market penetration. It is said to save 15% in travel delays and 8% in fuel consumption and emission even though the strategy did not contain any fuel consumption model [32]. MPC method is used to provide dynamic speed advice to individual vehicles considering the local and predictive traffic states. Since real-time detection and adjustment is not feasible in human-driven vehicles, this strategy is most suitable for automated vehicles (AVs). The future states of traffic lights were used to develop an optimization-based MPC model considering multiple objectives to compute the optimal speed that reduces idling time at red lights has been proposed in [33]. V2V communication is used to consider the signal status of the upcoming intersections to calculate the optimum vehicle control input to minimize fuel consumption by MPC method [34].

2.1.1. Categorization of longitudinal control methods

Optimal control problems have objective function which is minimized or maximised by sequentially choosing a set of actions that determine the behavior of a system. This leads to the selection of various types of optimal control problems. The optimal control problems are classified into three main categories: dynamic programming, indirect methods, and direct methods [35]. Dynamic programming is a method of splitting the given optimal control prob-

lem into a cluster of optimal control problems. The problems in the cluster are solved one by one in discrete time. *Kamalanathsharma et al* [36] proposed a eco-speed control strategy at signalized intersections using multi-stage dynamic programming. It resulted in about 19% fuel savings and 32% travel time savings in the vicinity of intersections. But the partial solutions obtained at each step should be kept in track at all times. *Nunzio et al* [37] also provided a solution to energy consumption minimization while driving through intersections using traffic signal information with dynamic programming. Indirect methods are based on first-order optimality conditions obtained from Pontryagin's minimum principle (PMP). *Jiang et al* [38] used PMP to develop an eco-approach at the signalized intersection which considered partially connected and automated vehicles environment. These methods help in obtaining a strong state and control trajectories. When solved using an indirect method, the optimal control problem is transformed into a two-point boundary value problem or multi-point boundary value problem which is solved using an appropriate boundary value solver. These methods are highly accurate for small scale problems but high dimensional systems satisfying the optimality conditions become critical. Indirect method problems the basic idea is to convert the optimal control problem into a nonlinear programming (NLP) problem. *Liu et al* [39] and *Qi et al* [40] used direct method for eco-driving at signalized intersection with an objective to minimize fuel consumption and travel time. Direct methods were also used in various approaches for vehicle trajectory planning (VTP) and eco-driving strategies [8, 41, 7, 42, 43, 44].The NLP problem can be solved both sequentially and simultaneously. These methods might require a nonlinear solver like *fmincon* which might be computationally expensive. But standalone nonlinear solver like CasADi, GUROBI, YALMIP, ACADO, etc can be used to reduce the computational time.

GLOSA approaches use simple advice algorithms to calculate the advisory speed to be communicated with the driver. *Stevanovic et al* [45] proposed a novel and simplistic method to derive the vehicle position and order in the vehicular queue based on kinematic formulas for speed and discharge headways/saturation flow rates. *Stebbins et al* [27] also proposed two advisory algorithms for reducing delay, travel time, and fuel usage. A novel time looping technique that identifies the leader of the platoon was also proposed in the research.

Learning-based algorithms were also used in trajectory planning and eco-driving using artificial neural networks (ANN) and deep neural networks (DNN) [46],[47]. These algorithms were also used for eco-approach and departure (EAD) and speed forecasting. *Hao et al* [48] used reinforcement learning (RL) along with dynamic programming for adaptive eco-driving strategy for actuated signals.

2.1.2. Input and operating conditions

Each control method has its assumptions, requirements, and operating conditions limited to their applications which make them distinct. Most of the eco-driving approaches consider that the vehicles capable of infrastructure to vehicle (I2V) communication get traffic signals and road information. *Zhao et al* [8] assumed that the information of position and speed of the following and preceding vehicles are available through the connected vehicle technology or roadside unit (RSU). They also considered that there was no communication delay or error in the cooperative platoon. *Wang et al* [41] assumed that there was no vehicle actuator

delay while considering the delay in communication. Most of the studies on energy-efficient driving or trajectory planning are focused only on longitudinal control [39, 5, 7, 40].

The algorithm requires data parameters to control the respective trajectory or perform the necessary action. Different eco-driving and trajectory control approaches require various information to calculate the desired trajectory or profile or advice. Signal and phase timing (SPaT) were used in various previous researches to get the information of current and future signal timings [39, 8, 41, 42, 40]. This information was used to predict or calculate an optimum speed profile that results in lower energy consumption and travel time. *Stebbins et al* and *Stevanovic et al* proposed GLOSA approaches that used SPaT together with instantaneous speed and acceleration values of the following and preceding vehicles to ensure that the equipped vehicle passes the intersection within the present or next to green phase [27],[45]. *Ye et al* [46] and *Wu et al* [47] proposed a eco-driving control method for intersections using neural networks which makes use of radar data along with SPaT and GPS interface device (GID) information. Dedicated short-range communication (DSRC) was also used for communication between the vehicles. *Hao et al* [48] used radar and camera data in addition to SPaT and GID. The learning-based algorithm also used the instantaneous speed and acceleration values of the equipped vehicles along with DSRC for communication.

2.1.3. Problem formulation

Different parameters are optimized to get different results. The desirable values of optimized parameters can be controlled by cost weights in objective functions. Optimal velocity and acceleration profiles lead to minimized fuel/energy consumption and travel time. *Liu et al* [39] formulated a nonlinear objective function including speed, acceleration, the maximum number of vehicles passing the intersection at that green phase, and fuel consumption. Linear inequality constraints were set on the states and bounded control input. The acceleration values are optimized in such a way that speed values are maximized for vehicles that could pass through the intersection and minimized speed values for vehicles that could not pass. This results in lesser fuel consumption values for vehicles that could not pass. *Zhao et al* [8] and *Jiang et al* [36] defined the objective function as a sum of terminal and running costs. The terminal cost was defined as the squared difference between the terminal states of the system and the desired terminal states. As the algorithm focused on minimizing the total fuel consumption of the platoon, the running cost was set as the driving cost at every time step. Zhao used an instantaneous fuel consumption model to capture fuel consumption at each time step. The control objective was achieved with the help of constraints on speed, acceleration, jerk, and safety. Optimal vehicle trajectory planning approaches for conventional vehicles work in such a way that it calculates the optimal speed profile with least energy consumption based on a family of piece-wise trigonometric-linear profiles. When the environment is partially automated the AVs are made to track the optimum speed profile. A quadratic cost function is defined with constraints on acceleration, headway distance, and jerk [41, 7, 42, 40]. *Qi et al* co-optimized vehicle dynamics and powertrain operations in addition to trajectory planning using a nonlinear constrained optimized problem [43]. A radial basis function neural network (RBF-NN) with a three-layered feedforward network is used instead of an optimal controller by *Ye et al* [46] for a prediction based eco-approach and departure at signalized intersections with speed forecasting on preceding vehicles.

2.1.4. Scenarios and Penetration rates

This research is focused on longitudinal control strategies for signalized intersections. Thus the number of traffic signalized intersections and signal timings play a vital role in the performance of the control algorithm. Some studies assume that the signal timings are fixed and known before the optimization. Signal timings can also be optimized for throughput and minimizing travel time. But adaptive signal timings or optimization of signal timings are not focused on this research. GLOSA approaches are highly dependent on signal timings as the optimal speed advisory is calculated using the instantaneous speed, acceleration of equipped, preceding and following vehicles and signal timings. Only fixed timing control approaches are considered in this research. The number of intersections the optimization has to look ahead also influences the computational load on the controller. Eco-driving approaches [8, 41, 42, 43] consider single isolated intersections. *Yang et al* [7] and *Liu et al* [39] considered both single and multiple intersection with and without queue effects scenarios in their research.

Penetration rates is another important factor that influences the performance of the control algorithm. *Liu et al*, *Qi et al* and *Homchaudhuri et al* considered a fully equipped and automated environment for their research. *Zhao et al* [8] developed a platoon based cooperative eco-driving model for mixed automated and human-driven vehicles at signalized intersections. It was found that when the penetration level is from low to moderate, the cooperation between automated vehicles (AVs) and human-driven vehicles (HVs) was beneficial for both fuel consumption and time. The research also reflects that a larger platoon size helps to achieve a stronger reduction in fuel consumption and stabilize traffic flow. Finally, when the penetration rate reaches 100% the performance improvement becomes trivial. *Wang et al* [41] demonstrated more than 7% reduction in energy consumption and up to 59% reduction in pollutant emission when all vehicles were equipped with the proposed controller. *Yang et al* used INTEGRATION microscopic traffic assignment and simulation software to conduct a comprehensive sensitivity analysis of system market penetration rate (MPR) along with other variables. The analysis showed that at 100% MPR, reduction in fuel consumption is as high as 13.8%. Car following models like Intelligent Driver Models (IDM) have been used to represent human-driven vehicles in a partially or mixed vehicle environment [38, 46, 8].

Various state of art longitudinal control methods were studied and reviewed in this section. It was found that most of the eco-driving and trajectory control strategies use optimal control methods. The types of optimal control methods such as dynamic programming, indirect control and direct control methods were studied. It was also observed that in most of the research approaches SPaT, V2V and V2I are assumed to be equipped by vehicles. A lot of focus has been given to optimization of fuel consumption in ICE vehicles when compared to optimization of energy consumption in electric vehicles. Nonlinear and quadratic objective functions were used to formulate the optimal control problem. The number of intersections and signal timing information play a vital role in optimization. It was also found that there is a significant reduction in fuel/energy consumption and travel time with an increase in penetration of vehicles equipped with eco-driving strategies or fully automated vehicles.

2.2. Overview of energy consumption models

For any type of vehicle, fuel/energy consumption is one of the major factors that will affect its growth in the market and also its performance. In this research, only electric vehicles are studied. Even though electric vehicles are becoming popular, a lot of work-related to electric vehicle technology has to be studied and developed. One such necessary area to be studied is the energy consumption of EV's. There are several works for fuel consumption models of ICE vehicles but not a lot of research is available on the EV energy consumption models.

2.2.1. Types of energy consumption models

Different energy estimation models for electric vehicles have been developed over the years by several researchers for various researches on energy-efficient driving. An EV energy consumption model explains the quantitative relationship between EV energy consumption rate and various impact factors. Different categories of models have been developed to capture this relationship as shown in figure 2.1 [40]. The analytical models are simple physical or mathematical models based on energy balance. The statistical models are data-driven models; they use regression methods or models to estimate energy consumption. Computational methods use artificial neural networks (ANN) and clustering methods to estimate the energy consumption of EVs. These models are also used in predicting the energy consumption of EVs before the commencement of the trip, with the help of available traffic and road information.

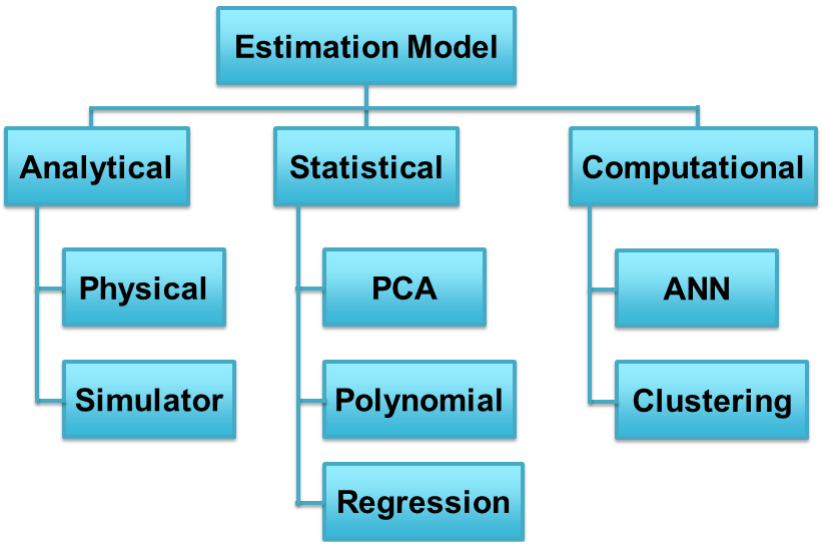

Figure 2.1. – Classification of Energy consumption models

Based on the granularity, the research on energy consumption models is carried out in three levels: macroscopic, mesoscopic, and microscopic respectively. Regional energy consumption of transportation is usually studied with the help of macroscopic methods. Macroscopic models assume that all vehicles travel at an average speed and distance. The variation in the second-by-second speed profiles and driver behavior are ignored. On the other hand, mi-

croscopic methods are based on estimating the energy consumption of individual vehicles. This method is more accurate than the former but they usually depend on large vehicle-specific and trip-specific characteristics [49]. Mesoscopic methods are based on computing road link wide energy consumption providing a balance between less accurate macroscopic methods and data-intensive microscopic methods, proving to be suitable for practical applications. Even though mesoscopic methods only require limited input parameters, they are suitable for conventional ICE vehicles only as the required data is obtained from the chassis dynamometer. This is due to the inability of the chassis dynamometer to reflect real-time characteristics of EV's such as regenerative braking which plays a vital role in the estimation of energy consumption in EV's [50].

2.2.2. Modelling orientation/causality

Usually, energy consumption models are modeled in two ways based on the method of calculating energy consumption: forward-facing and backward-facing [51]. The backward-facing approach does not contain a driver model. This approach is used when the speed profile with respect to each time step is given. The force required to accelerate the vehicle is calculated, then the force is converted to torque in the upstream component directly. Thus the calculation travels from the wheels to powertrain opposite to the actual tractive power flow direction until the energy consumption required to meet the speed trace has been computed as shown in figure 2.2. The backward-facing approach is adopted for its quick execution speed which allows it to be used for component level efficiency testing in industries. The nature of efficiency/loss calculation allows very simple integration routines to be used with relatively large time steps of the order of 1s. The drawback of the backward-facing approach is that it is not well suited for dynamic conditions like exceeding the capabilities of the drivetrain since it is assumed that the vehicle already meets the given speed trace [52].

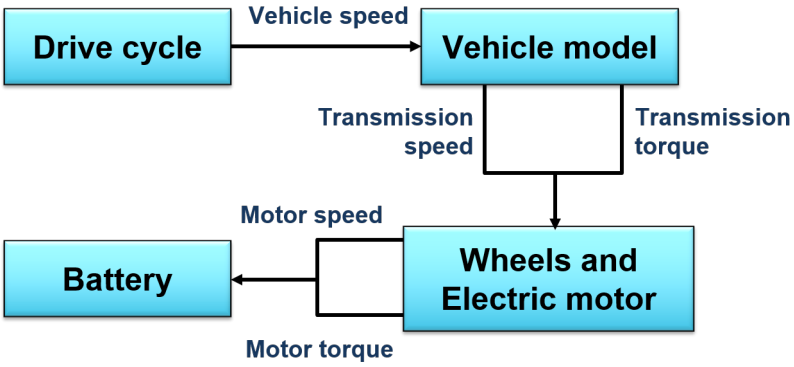

Figure 2.2. – Backward facing model

Forward-facing approach differs from the former by including the driver model (usually a PI controller) to trace the given speed profile by giving out the appropriate throttle and brake commands. The throttle output by the driver model is converted to torque given out

by the engine which is again fed as input to the transmission until the tractive force of the tires is calculated to accelerate the vehicle. This approach is usually used in hardware development and detailed control simulation. Forward-facing approaches are mostly used in vehicle simulators and controllers where the inputs are actual control signals and true torque values. It can overcome the drawback of the backward-facing model easily by handling dynamic conditions. The only drawback of the forward-facing models is its execution time and simulation speed. Since it deals with real-time inputs, higher-order integration schemes are adopted using small time steps. Even though the results are more accurate and stable, the simulation is time-consuming for early design stages.

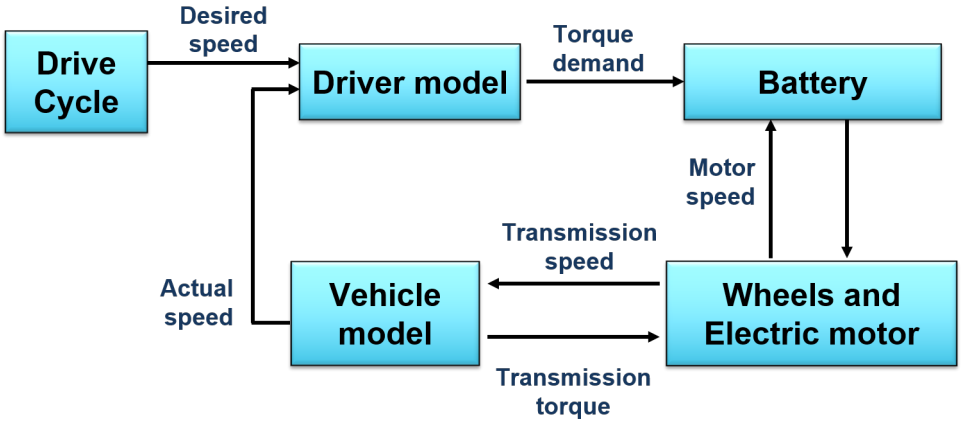

Figure 2.3. – Forward facing model

2.2.3. Factors influencing the model

- Granularity: As mentioned earlier in this section, granularity represents the scale of the model such as macroscopic, mesoscopic, and microscopic. The microscopic models are used to calculate the second-by-second or instantaneous energy consumption as they require detailed energy-efficient velocity profile planning. [53, 54, 55, 56, 57]. Trip based or macroscopic models were also used for some researches which involved applications such as estimation of energy consumption for a particular trip or journey [58, 59, 60, 61, 40]. Link-based or mesoscopic energy estimation models were also developed to determine the total energy consumed for roadway network link [62]. The scale of the model has a direct impact on the accuracy of the energy estimation model. *Cauwer et.al* proposed a hybrid estimation model consisting of both microscopic and mesoscopic models that are required to compute energy consumption at different granularities simultaneously for sophisticated applications [63].

- External impact factors: These are factors that affect the energy estimation models externally other than vehicle's internal factors such as powertrain, efficiencies, etc. Four main external factors have an impact on the estimation model such as 1) factors related to traffic conditions that indirectly affect the vehicle dynamic parameters such as speed and acceleration. *Abousleiman et al* presented an energy consumption model

taking into account the possible effects of traffic on various routes [59]. 2) Factors related to infrastructure such as road inclination, road surface also influences the energy estimation. *Wu et al, Zhang et al* propose estimation models taking into account the influence of roadway grade and the choice of route[58, 57]. *Wang et al* [64] developed a model that can estimate and predict the energy consumption based on the available road information using an offline algorithm. It was found that the offline algorithm can give an accurate energy consumption estimation to the driver before a trip begins and also results in an optimal choice of fastest and economic speeds. 3) Ambient temperature also plays a major role in EV energy estimation as batteries are influenced by operating temperatures. It was found that some amount of energy is lost due to ambient temperature based on two factors: the cabin heat energy and battery conditioning energy [59]. Thus a constraint is placed on the operating ambient temperature to ensure that its state of charge (SOC) remains high. But to maintain the optimum temperature of the batteries the OEM's had to install a liquid cooling/heating system which not only increased the price tag but also increased the auxiliary load power. 4) Driving behavior is the most important factor of all. It includes the way of driving such as driver aggressiveness, brake, pedal position/pressure and driving mode selection. In most of the models, this is reflected by the drive cycle input to the model [60, 61, 64]. *Wu et al* proposed an analytical electric power consumption model as a function of instantaneous speed and acceleration profile for eco-driving application at intersections [58].

- Internal impact factors: These are internal factors such as efficiencies, powertrain working, and auxiliary loads. The EV characteristics that affect the model are studied by numerous researches [53, 54, 60]. The vehicle characteristics differ from vehicle to vehicle. The energy estimation model accuracy is also dependent on the efficiencies of the vehicle such as motor efficiency, transmission efficiency, battery efficiency, etc. The auxiliary loads are loads contributes by the components such as air conditioning, heating, and ventilation systems, etc. These systems typically contribute to about 500-700 W of power rating [53, 60, 61, 55]. Auxilary load affects the estimation as they are always on even when the vehicle is not in motion. Some researches tried to reduce this effect by implementing a constraint on the auxiliary loads [59].

- Regenerative braking: Since all EVs have the ability of regenerative braking, it is one of the important factors that affect the energy estimation. In earlier researches, regenerative braking was included as a factor in the range of 0.5-1 when calculating the regenerative power [59, 60, 40, 56]. Regenerative braking is indirectly influenced by the deceleration pattern or driving behavior of the vehicle. *Fiori et al* [53] proposed an analytical instantaneous energy estimation model for PHEV's. A novel approach of capturing the instantaneous braking energy regeneration as a function of vehicle deceleration was introduced. It resulted in a more realistic model with an average error of 5.9% relative to empirical data. *Yang et al* [57] added battery properties as a factor to the same approach in estimating the energy consumption of car-following models. *Wang et al*[64] used different control strategies for regenerative braking such as parallel regenerative braking control strategy based on brake pedal travel and one-pedal driving control strategy based on releasing the acceleration pedal. It was found

that the regenerative braking strategy improves the braking feel and energy efficiency. The simulation results proved that the energy estimation model was able to calculate the energy consumption with an error smaller than 5% for different circumstances.

2.2.4. Validation of the models

The validation of energy consumption models is a very important aspect. From the literature, it was found that the models are either validated through real-time testing where the calculated data is compared with the empirical data from the experiment and simulations in which testing scenarios are designed in a dedicated simulation tool to simulate the developed model. Experimental validation is very accurate but they consume a lot of manpower, time, and money. They are also dependent on the necessary infrastructure, weather conditions, and logistics. On the other hand, simulations are easier to check the working of the models. They are easy to control and collect data. They require computational power and proper input data. Various scenarios can be designed to obtain the necessary outputs. The limitation of simulations is that they are far from real-time testing. Sometimes simulator experiments lead to discomfort and unrealistic driving. *Fiori et al* [53] validated the power-based analytical EV energy consumption model using experimental data on EV consumption levels that were collected by Joint Research Centre (JRC) of the European Commission (2015) and Idaho National Laboratory (INL) in the AVTA program of the United States Department of Energy (U.S.DOE)(2013). *Wu et al* [58] validated the analytical EV power estimation model using approximately 5 months of EV data which was recorded from a test vehicle built for the research. The data was used to analyze the EV characteristics, driver behaviors, and route choices. *Abousleiman et al, Qi et al and Wang et al* [59, 40, 64] also validated their models with experimental data. Other models were validated with available EV data from the manufacturers and literature using simulations [54, 60, 61]. This validation effort was limited due to the energy data availability of EVs [56, 57].

2.3. Literature gaps

Even though platooning is a familiar concept in highways, when coming to the urban roads they have to overcome a lot of barriers. Urban roads contain signalized intersections. The vehicles at the vicinity of the intersection have to slow down and stop in front of traffic signals and then accelerate to the final velocity from start. This leads to longer idling time and irregular acceleration/deceleration maneuvers which in turn results in higher fuel consumption, emissions, longer travel time, and delay. Energy consumption and travel time are the two main parameters that should be optimized. As a result of the literature study, it was found that there is a need for a simple, realistic, and generic instantaneous energy consumption model for EVs. It was also found that only very few control strategies were focused on minimizing energy consumption and travel time together for the whole platoon. Flexible control strategies in which the scope can be extended to multiple intersections, queue effects, and mixed environment are vital. It is also found that the advised optimal speed profiles are often not tracked perfectly by the drivers [65], leading to a decrease in energy efficiency, an increase in travel time, and sometimes increased speed. This also calls in for a automated vehicle model to track the optimal speed profile eliminating the driver.
The need, significance, and types of vehicle dynamics and energy consumption models with

their merits and demerits were discussed. It was found that vehicle dynamics models like point mass were used to model simple vehicles for representing traffic behavior and simulations. BEVs were found to be simple in modeling and better for urban transportation. Even though they fall short in range, it can be increased with the help of energy-efficient trajectory planning and control approaches. Although numerous researches have focused on modeling EV energy consumption models, these studies were limited to their application of control algorithms. A simple, accurate, and efficient energy consumption model is needed to develop real-time eco-driving and optimal trajectory control strategies. Factors such as regenerative braking, driving behavior, and auxiliary loads were found to have a direct impact on the estimation of energy consumption. It was also found that validating the model through simulations widens the scope of testing by setting up appropriate scenarios and can save time. However, validating through simulations might compromise the accuracy of the models.

As a step in addressing these gaps, in this research a simple and flexible control algorithm for energy efficient vehicle platooning at signalized intersections is proposed. A battery electric vehicle model for tracking the optimal advise from the controller is also modelled. The Virginia Tech Comprehensive Power based Energy consumption Model (VT-CPEM) is adapted for the energy consumption model due to its simple, accurate and flexible nature.

3. Controller design

The literature study in Chapter 2 has shown how eco-driving methods for signalized intersections can be modelled and what effects it may have on the performance of the platoon. Various energy consumption models were also discussed to determine which model can be used for calculating instantaneous energy consumption in the controller design. The next steps are to design the optimal controller for energy-efficient driving at signalized intersections.

Therefore, this chapter starts with defining the control objectives to be fulfilled in section 3.1 followed by the optimization problem formulation in section 3.2. The energy consumption model used in the optimization is explained in section 3.3. The modeling of the regenerative braking effect for electric vehicles is also addressed in this section. The solution approach with the solver is briefed in section 3.4. Finally, the tuning parameters of the controller are discussed along with the constant parameters in section 3.5.

3.1. Control Objective

The optimal control strategy presented in this chapter is expected to fulfill a set of control objectives. Firstly to minimize the travel delay of the vehicles that pass through the intersection during green phases by maximizing the vehicle speeds. Next to minimize the energy consumption of vehicles that could not pass through the intersection during the green phase and the following red phase. Finally, to minimize the accelerations of all the vehicles to maximize driving comfort. Also, the maximum number of vehicles that can pass through the intersection is expected to be optimized. The safety of all vehicles should also be satisfied on all occasions of driving.

3.1.1. Design assumptions

- The road section chosen for this research is an isolated signalized intersection.
- The signal timings are fixed and assumed to be known in prior to the optimization.
- All the vehicles in the platoon are considered to be equipped with Vehicle to Vehicle (V2V) and Vehicle to Infrastructure (V2I) communication technologies.

3.2. Optimization problem

An optimal control problem (OCP) is set up which minimizes a cost function (J) subject to the system dynamics and constraints ($G(\mathbf{x}, \mathbf{u})$) to obtain the optimal control sequence ($\mathbf{u}$).

The general structure of a optimal control problem at initial state x_0 is given in equation 3.1 along with the constraints in equation 3.4.

$$min_u J(\mathbf{x}, \mathbf{u}, t) \tag{3.1}$$

The cost function can be stated as

$$J = \int_0^T g(\mathbf{x(t)}, \mathbf{u(t)})dt + g_T(\mathbf{x(T)}) \tag{3.2}$$

where $g(\mathbf{x(t)}, \mathbf{u(t)})dt$ is the running cost or stage cost and $g_T(\mathbf{x(T)})$ is the terminal or final cost. T represents the final time of optimization. The general state dynamics can be denoted by the relation:

$$\dot{x} = f(\mathbf{x(t)}, \mathbf{u(t)}) \tag{3.3}$$

$$G(\mathbf{x}, \mathbf{u}) \leq 0 \tag{3.4}$$

3.2.1. System Dynamics

The system dynamics consists of all the states and inputs of the designed optimal controller. The control input $\mathbf{u}$ of the OCP is accelerations of all vehicles, $a_i(t)$. Longitudinal position, $x_i(t)$ and speed, $v_i(t)$ of the controlled vehicle are treated as the state variables $\mathbf{x}$. i represents the vehicle sequence number in the platoon. The total number of controlled vehicles is denoted by N and t represents the particular time instant. The state and control input vectors are shown as

$$\mathbf{x} = (x_1(t), \ldots, x_i(t), \ldots, x_N(t), v_1(t), \ldots, v_i(t), \ldots, v_N(t))^T \tag{3.5}$$

$$\mathbf{u} = (a_1(t), \ldots, a_i(t), \ldots, a_N(t))^T \tag{3.6}$$

An ordinary differential equation is used to represent the longitudinal dynamics model, given as

$$\frac{\mathrm{d}}{\mathrm{d}t}\mathbf{x} = \frac{\mathrm{d}}{\mathrm{d}t}(x_1(t), \ldots, x_i(t), \ldots, x_N(t), v_1(t), \ldots, v_i(t), \ldots, v_N(t))^T = \mathrm{f}(\mathbf{x}, \mathbf{u}) \tag{3.7}$$

The state equation of continuous time system is described in the form :

$$f(\mathbf{x}, \mathbf{u}) = A\mathbf{x} + B\mathbf{u} \tag{3.8}$$

$$A = \begin{bmatrix} A_0 & A_1 \\ A_0 & A_0 \end{bmatrix}^{2N \times 2N} ; B = \begin{bmatrix} A_0 & 0 \\ A_1 & 0 \end{bmatrix}^{2N \times N} \tag{3.9}$$

$$A_0 = \begin{bmatrix} 0 & 0 & \cdots & 0 \\ 0 & 0 & \cdots & 0 \\ \vdots & \vdots & \ddots & \vdots \\ 0 & 0 & \cdots & 0 \end{bmatrix}^{N\times N} ; A_1 = \begin{bmatrix} 1 & 0 & \cdots & 0 \\ 0 & 1 & \cdots & 0 \\ \vdots & \vdots & \ddots & \vdots \\ 0 & 0 & \cdots & 1 \end{bmatrix}^{N\times N} \tag{3.10}$$

3.2.2. Cost function

The cost function (J) to be minimized is formulated with both the state and control variables. The formulation of cost function is inspired from [66] in which it was formulated for ICE vehicles while this research focuses on electric vehicles. Thus a energy consumption model is formulated in section 3.3. The control problem at an isolated signalized intersection is given by two scenarios based on the prediction horizon (T). One, for a single signal cycle (i.e) one green and one red phase as shown in equation 3.11 and the second having an extended prediction horizon or signal phase (i.e) an additional green phase following the first signal cycle as shown in equation 3.12. For both the scenarios, the intersection is isolated without any queue. The prediction horizon is defined as a sum of green phase (g_i) and red phase (r_i) signal timings $T = g_i + r_i$. The cost function consists of four individual functions such as acceleration $a_i(t)$, speed $v_i(t)$, the maximum number of vehicles q that could pass the stop-line, and instantaneous energy consumption rate $e_v(t)$. The instantaneous energy consumption rate in kWh/s is expressed as a function of acceleration and vehicle speed. The cost weights are denoted by $\beta_1, \beta_2, \beta_3, \beta_4$ and β_5 for each term in the cost function respectively. All the parameters used in the controller design are explained in section 3.5.3. Two scenarios are formulated in order to evaluate the performance of the automated platoon under single and multiple signal cycles.

Scenario 1: Vehicles stopping at intersection - one signal cycle

$$\min_{\mathbf{u},\boldsymbol{q}} \boldsymbol{J} = \min_{\mathbf{u},\boldsymbol{q}} \int_0^T \left(\boldsymbol{\beta}_1 \sum_{i=1}^{N} a_i^2(t) - \boldsymbol{\beta}_2 \sum_{i=1}^{q} v_i(t) - \boldsymbol{\beta}_3 q + \boldsymbol{\beta}_4 \sum_{i=q+1}^{N} e_v(v_i(t), a_i(t)) \right) d\mathbf{t} \tag{3.11}$$

The cost function for this scenario is formulated for the number of vehicles q passing the intersection with maximal speeds, and with minimal energy consumption rates for vehicles that could not pass the intersection. The speed is maximized only for q vehicles in order to make sure the respective vehicles pass through the intersection at maximum speed decreasing the travel delay. The acceleration term in the cost function is responsible to maintain driving comfort for all vehicles throughout the prediction horizon. There is no terminal cost present in the cost function because it is same as the running cost, and the desired results were obtained with the running cost itself.

Scenario 2: All vehicles passing the intersection - extended prediction horizon

$$\min_{\mathbf{u},q} \boldsymbol{J} = \min_{\mathbf{u},q} \int_0^T \left(\boldsymbol{\beta}_1 \sum_{i=1}^{N} a_i^2(t) - \boldsymbol{\beta}_2 \sum_{i=1}^{q} v_i(t) - \boldsymbol{\beta}_3 q + \boldsymbol{\beta}_4 \sum_{i=q+1}^{N} e_v\left(v_i(t), a_i(t)\right) \right) dt \\ -\boldsymbol{\beta}_5 \int_{g_1+r}^{T} \left(\sum_{i=q+1}^{N} v_i(t) \right) dt \tag{3.12}$$

In this scenario, the cost function is formulated to make the vehicles that could not pass the intersection $(N-q)$ in the first green phase g_1 to pass through in the second green phase g_2. The inclusion of the second green phase g_2 results in the increase in prediction horizon $T = g_1 + r_1 + g_2$. The cost function also consists of a fifth-term denoting the speed of the $(N-q)$ vehicles in g_2. This term allows the vehicles that could not pass the intersection in g_1 to pass the intersection with maximum speeds at the start of g_2. The last term is not included in the full prediction horizon as, these vehicles do not pass the intersection at the first green phase, so their energy consumption is minimized. They are allowed to maximize their speeds while departing the intersection in the next green phase.

The variable q in both the scenarios should also be optimized. The threshold value for the maximum number of vehicles that can pass through the intersection is defined by M, which is obtained with the following relation:

$$M = ceil\left(\frac{g_1 - L_0/v_{max}}{t_{min}}\right) \tag{3.13}$$

In the above equation, g_1 is the first or current green phase timing, L_0 is the position away from the intersection where the optimization starts. v_{max} denotes the maximum speed limit of the platoon and t_{min} denotes the minimum safe car-following time gap between the vehicles in the platoon. Thus q $(q \leq M)$ cannot be more than the value of M, which also makes it a constant term in the cost function. The parameter q is optimized by selecting the maximum number of vehicles that could pass the intersection in the current green phase. Since the term q is a constant in the objective function, it is not affected by the cost weight β_3. The signal phase timings play a vital role in the value of q. The vehicles are expected to pass the intersection only at the green phase as there is a position constraint for the vehicles during the red phase.

3.2.3. Constraints

One of the advantages of using an optimal controller is its ability to handle the constraints on the dynamic system. The controller has certain constraints that the optimal control problem has to satisfy. Both states and control input are subjected to the below constrained equations.

- Permissible acceleration: It is the allowable range of acceleration between the maximum acceleration, a_{max} and the minimum acceleration, a_{min}

$$a_{\min} \leqslant a_i(t) \leqslant a_{\max} \tag{3.14}$$

The maximum acceleration is considered to be a constant as the friction and road parameters are assumed to be constant. Here, i corresponds to the vehicle number in the platoon and t ranges from 0,1...,T-1. Therefore, the total number of design variables in the optimal control problem is i*T.

- Speed: This constraint acts to restrict the vehicle speed $v_i(t)$ to the maximum speed limit of v_{max}. The speed values are always expected to be non-negative to avoid reverse vehicle travel.

$$0 \leqslant v_i(t) \leqslant v_{\max} \tag{3.15}$$

- Safety/No-collision constraint: The controlled vehicles are required to maintain safe time gap and space gap which should be greater than or equal to the minimum safe gap throughout the prediction horizon.

$$x_i(t) - x_{i+1}(t) \geqslant v_{i+1}(t)t_{\min} + s_0 + l \tag{3.16}$$

where $x_i(t)$ is the rear bumper position of the preceding vehicle at a time instance, $x_{(i+1)}(t)$ is the position of the immediate following vehicle at a time instance, t_{min} is the minimum time gap of the controlled platoon, s_0 is the minimum space gap of the controlled platoon in stationary conditions and l is the length of the standard vehicle. In equation 3.16, it can be seen that the preceding vehicle or the leader vehicle in the platoon is not subjected to the constraints. This is modified if there is a queue present in the upstream intersection. The leader vehicle has to satisfy the safety constraint with the last vehicle in the queue present at the intersection.

- Position constraint: The green and red phase timings along with the stop line position at the intersection are used to identify whether the vehicles can pass the intersection. Specifically red phase timings act as the position constraints as they restrict the vehicles from passing the intersection. For the scenarios in section 3.2.2, considering single isolated intersection, there is only one red phase constraint. The longitudinal position of the qth vehicle should be greater than or equal to 0 at the end of green phase g_1 in the first intersection. The remaining vehicles in the platoon $q+1$ to N which could not pass the intersection are constrained to stop behind the stop-line during the red phase, meaning the longitudinal position of the $q+1$ to N vehicles within the red phase should be less than or equal to 0 (stop-line). The constraints are expressed as follows:

$$\begin{aligned} &x_q\left(t = g_1\right) \geqslant 0 \\ &x_i\left(g_1 \leqslant t \leqslant g_1 + r\right) \leqslant 0 \quad q+1 \leqslant i \leqslant N \end{aligned} \tag{3.17}$$

For scenario 2 in section 3.2.2, the $q+1$ to N vehicles are expected to pass through the intersection in the second green phase g_2 which means that the longitudinal position

of the vehicles $q+1$ to N should be greater than or equal to 0 (stop-line) in the second green phase.

$$x_{q+1:N}\left(t = g_1 + r_1\right) \geqslant 0 \tag{3.18}$$

3.3. Energy consumption model

The Virginia Tech Comprehensive Power-based EV Energy Consumption Model (VT-CPEM) is a simple, accurate, and efficient model to calculate the instantaneous energy consumption of EVs. Acceleration and speed values are used as inputs to the energy consumption model. The VT-CPEM is chosen due to its simplicity and flexibility it can be easily integrated with complex frameworks such as microscopic traffic simulation models and in-vehicle applications. The model can be easily calibrated using the publicly available EV data without the need for field data collection. VT-CPEM also accounts for regenerative braking efficiency in EVs as a function of vehicle deceleration. Auxiliary loads in the vehicle such as air conditioning, heating, and ventilation are also considered when estimating energy consumption.

It is a backward-facing power-based model. The fact that it computes the tractive effort at the wheels and progresses backward towards the electric motor and battery makes it a backward-facing model [67]. Backward facing models are simple and faster in execution [68].

3.3.1. Model formulation

Since it is modelled using the backward approach, first, the power in the wheels is calculated using the following equation

$$P_{\text{wheels}}\left(t\right) = \left(ma(t) + mg \cdot \cos(\theta) \cdot \frac{C_r}{1000}\left(c_1 v(t) + c_2\right) + \frac{1}{2}\rho_{\text{Air}}\, A_f C_D v^2(t) + mg \cdot \sin(\theta)\right) \cdot v(t) \tag{3.19}$$

Next, the power in the electric motor P_{mot} is computed using the electric motor efficiency η_m, driveline efficiency η_d and battery efficiency η_b in traction mode. The power in the traction mode is assumed to be positive as the power flows from the motor to the wheels. The power in the electric motor during braking mode or regenerative mode is calculated using the regenerative braking efficiency η_{rb}. The power in the braking mode is assumed to be negative as the power flows from the wheels to the motor.

$$P_{mot} = \begin{cases} P_{wheels}/(\eta_d \times \eta_m \times \eta_b) & \forall a(t) \geqslant 0, \quad \text{Traction mode} \\ P_{wheels} \times \eta_d \times \eta_m \times \eta_b \times \eta_{rb} & \forall a(t) < 0, \quad \text{Braking mode} \end{cases} \tag{3.20}$$

$$P_{mot.net} = P_{mot} + P_{auxiliary} \tag{3.21}$$

The net power is calculated as a sum of motor power P_{mot} and auxiliary power $P_{auxiliary}$. Finally the total energy consumption (EC) is calculated by integrating the total net power over time as follows

$$EC\left[\frac{\text{kWh}}{\text{s}}\right] = \frac{1}{3,600,000} \cdot \int_0^t P_{mot.net}(t)dt \tag{3.22}$$

3.3.2. Regenerative braking efficiency as a function of deceleration

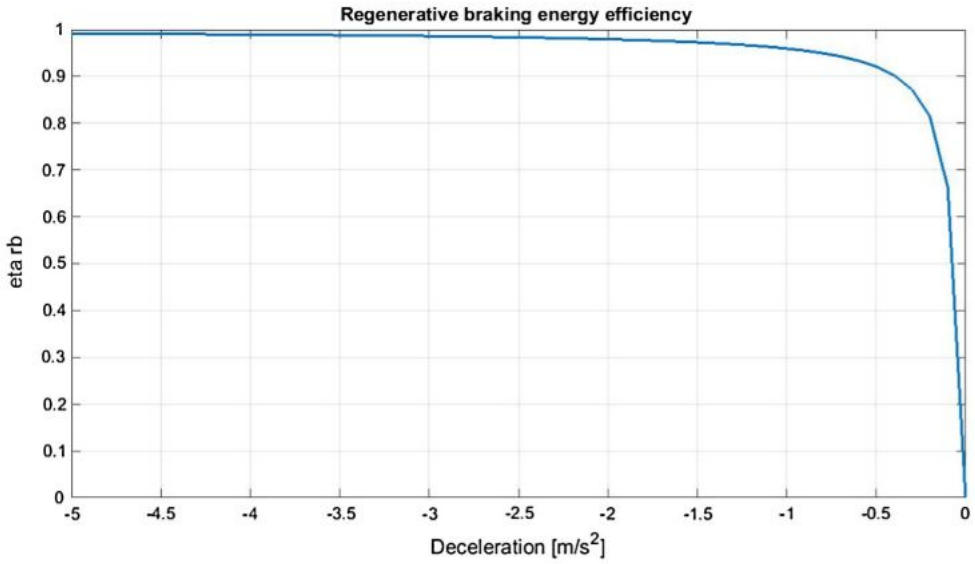

Figure 3.1. – Instantaneous regenerative braking as a function of deceleration

Regenerative braking is one of the main unique features of EVs. Its ability to produce and store energy during deceleration makes EV one step ahead of conventional ICE vehicles. $P_{mot.net}$ value is a sum of positive power from the motor and the negative power to the motor. When the vehicle is in traction mode the energy flows from the powertrain (i.e) electric motor to the wheels. In this case, the power in the electric motor is higher than the power in the wheels. And the power in the wheels is assumed to be positive ($P_{wheels} > 0$). On the contrary, when the vehicle is decelerating or braking the power flow is from the wheels to the electric motor. The power in the wheels is higher than the power in the motor and also the power is assumed to be negative ($P_{wheels} < 0$). Thus making the power in the motor also negative, which shows that the motor rotates in the opposite direction, charging the battery as a inverter. During this phase, the braking system of the vehicle dissipates kinetic energy and there is no driving power. The relation between the regenerative braking efficiency η_{rb} and negative acceleration $a^{(-)}$ is found to be exponential as illustrated in figure 3.1. The regenerative braking efficiency is calculated instantaneously as a function of

negative acceleration of the vehicle using the following relation.

$$\eta_{rb}(t) = \begin{cases} \left[e^{\left(\frac{0.0441}{|a(t)|}\right)}\right]^{-1} & \forall a(t) < 0 \\ 0 & \forall a(t) \geqslant 0 \end{cases} \tag{3.23}$$

The parameters and coefficients used for the energy consumption modelling is given in table A.1. The formulation and parameters used for energy consumption model is adapted from [69].

3.4. Solution approach

Optimal control is a mathematical optimization method that finds a control for the dynamical system over a period of time by optimizing a objective function. The method of solving an optimal control problem (OCP) can be categorized into three ways such as Dynamic Programming (DP), indirect optimal control and direct optimal control. Dynamic programming is a method of splitting the given optimal control problem into a cluster of optimal control problems. The problems in the cluster are solved one by one in discrete time. Indirect methods are based on first-order optimality conditions obtained from Pontryagin's minimum principle (PMP). Direct method problems convert the optimal control problem into a nonlinear programming (NLP) problem or a discrete constrained minimisation problem. The problem discussed in this research is bounded, convex and has a continuous objective function with nonlinear system dynamics and linear constraints.

The optimal control problem defined in section 3.2 is continuous in time. The problem is solved using the direct optimal control method (i.e) transforming the optimal control problem into a nonlinear programming problem (NLP) by discretizing the control variable (accelerations) within the prediction horizon. Zero order hold is used to discretize the continuous time signal by holding each sample for one sample interval. The inequality constraints for the NLP are chosen and transcribed from the earlier sections. The equality constraint is expressed using the system dynamics in equation 3.8. The linear inequality constraints are denoted by the constraints on state and control variables as in section 3.2.3. This optimal control problem is solved with CasADi toolkit in MATLAB interface using the sequential quadratic programming (SQP) algorithm. The general NLP is defined as follows

$$\begin{aligned} &\min_{y} f(y) \\ &\text{s.t.} \quad y_{lb} \leq y \leq y_{ub} \\ &h(y) \leq 0 \\ &g(y) = 0 \end{aligned} \tag{3.24}$$

In the above equation y is the decision variable, y_{lb} is the lower bound of y, and y_{ub} is upper bound of y. $h(y) \leq 0$ represents the inequality constraints and $g(y) = 0$ denotes the equality constraints.

3.4.1. CasADi

CasADi is an open source software tool for numerical optimization in general and symbolic framework for nonlinear programming [70]. The tool has a strong focus on optimal control (optimization involving differential equations) in particular. CasADi is not a standard optimal control problem solver but a interface that allows the user to build and implement their own optimal control problem solvers efficiently by providing a set of building blocks.

3.4.2. Sequential Quadratic Programming

SQP is one of the most successful iterative methods for numerical solution of a constrained nonlinear optimization problem. It is very effective and can be applied to problems with linear and nonlinear constraints. The SQP models the given NLP for every iteration by a Quadratic Programming (QP) subproblem. It solves the sub-problem and then uses the solution of the QP sub-problem to construct the new iteration. A detailed explanation of SQP working is given in Appendix B. QP OASES is the NLP solver used in this thesis.

Table 3.1. – Solver settings

Parameter	Settings
Hessian approximation	exact
Maximum no of iterations	100
Minimum step size	1e-10
Tolerance value	1e-6

The hessian approximation setting is set to "exact" as the objective function is at least twice differentiable throughout the optimization. The maximum number of iterations is changed to 100 from the default value of 50. Further increasing the iterations did not result in major change in optimized values of accelerations. The minimum step size and tolerance values were chosen as the solver's default values.

3.5. Tuning parameters

Finally, the controller should be tuned for best performance. The performance of the controller is hugely dependent on the prediction horizon and cost weights of the objective function. The prediction horizon also has a direct effect on the computational effort of the controller.

3.5.1. Prediction horizon

The prediction horizon T in this thesis is defined by the signal cycle timings as $T = g_i + r_i$. The amount of time required to display all phases for each direction of an intersection before starting over again is called the signal cycle length. The cycle length varies depending on the type of intersection like isolated, single lane or multilane and area of intersection like

urban or highway. The optimum signal cycle timing is also responsible for the efficiency of the intersection. Most commonly used signal cycle timings range from one minute to three minutes. The signal cycle is split into different phases of green, red and yellow. This thesis will only focus on red and green phases. A split of green phase $g_1 = 30s$ and red phase $r_1 = 30s$ is considered throughout the thesis. Thus the prediction horizon T is set to $T = 60s$ for scenario 1 which consists of one signal cycle and $T = 90s$ for scenario 2 which consists of an extra green phase. Split of the cycle also plays a vital role as g_1 is used to calculate the maximum number of vehicles that can pass the intersection in the current green phase. For the continuous time OCP to be solved as NLP, the continuous time model has to be discretized. The sampling time of the controller is set to $T_s = 1s$. If the sampling time was set smaller than 1s, it was found that the computation was faster but causes disturbance in convergence. On the other hand, if sampling time is larger it leads to convergence but computational time was very high. The influence of prediction horizon can be studied with the simulation results of scenario 1 and 2 in chapter 5.

3.5.2. Cost weights

The OCP also requires the cost weights in the objective function to be defined. There are individual cost weights for each function in the objective function namely $\beta_1, \beta_2, \beta_3, \beta_4$ for acceleration m/s^2, speed m/s, no of vehicles passing q veh and energy consumption rate kWh/s. For scenario 2, an additional cost weight β_5 is used for speed m/s of the vehicles that are expected to pass the intersection during g_2 with maximum speed v_{max}. The initial baseline weights are tuned by a special scenario, where the effect of all cost terms can be seen for all the N vehicles within the prediction horizon. Thus the objective function of scenario 1 in section 3.2.2 is modified as given

$$\min_{\mathbf{u},\boldsymbol{q}} \boldsymbol{J} = \min_{\mathbf{u},\boldsymbol{q}} \int_0^T \left(\boldsymbol{\beta}_1 \sum_{i=1}^{N} a_i^2(t) - \boldsymbol{\beta}_2 \sum_{i=1}^{N} v_i(t) - \boldsymbol{\beta}_3 q + \boldsymbol{\beta}_4 \sum_{i=q+1}^{N} e_v(v_i(t), a_i(t)) \right) d\mathbf{t} \quad (3.25)$$

The idea of tuning the weights by a special scenario is adapted from [66]. All the cost weights are initially set using the idea that smaller the desired error the larger the cost weight. Therefore, increasing the weight for a particular cost term states that more attention is given to control the particular term when compared to the others. Once the effect of the all the cost terms is evident, the controller is fine-tuned using various simulations by varying the cost weights and achieving the desired performance. The simulations led to the following observations,

- Variation in cost weight for q does not have any effect on the optimal solution.
- Different weights for acceleration and speed led to degraded controller performance.
- An increase in speed weights led to increase in energy consumption of the vehicles.
- Decreased weights for acceleration led to unsteady acceleration pattern resulting in driver discomfort.

- A very high weight for energy consumption led to lower speeds for the vehicles passing the intersection.
- Very small speed weights led to delay in reaching maximum speeds.

3.5.3. Parameters/Coefficients

Table 3.2. – Parameter and coefficient values of the controller

Notation	Parameter/coefficient	Value	Unit
N	Total number of vehicles in the controlled platoon	10	-
g_1	First green phase at intersection	30	s
r_1	First red phase at intersection	30	s
g_2	Second green phase at intersection	30	s
l	Length of vehicles in the controlled platoon	3	m
L_0	Distance away from the intersection stop-line in downstream direction to the point where the optimization starts	200	m
t_{min}	Minimum safe car-following time gap	2	s
s_0	Minimum safe space gap at standstill conditions	2	m
v_{max}	Maximum speed allowed at the single lane intersection	15	m/s
a_{max}	Allowable maximum acceleration	2	m/s^2
a_{min}	Allowable minimum acceleration	-5	m/s^2
	Initial speed of the driving platoon	8	m/s
	Initial space gap in the driving platoon	21	m
T_s	Time step	1	s
T	Prediction horizon	60,90	s
β_1	Cost weight for acceleration	0.5	-
β_2	Cost weight for speed	0.5	-
β_3	Cost weight for q	0.5	-
β_4	Cost weight for energy consumption rate	0.5	-

4. Vehicle model

The previous chapter explains about the controller design and solver used. Now, an electric vehicle model is required to track the optimal speed profile from the controller. The design of the longitudinal electric vehicle model is explained in this chapter. The chapter starts by laying out the assumptions and considerations of the designed vehicle model. This is followed by description of various subsystems such as brakes, vehicle body, driveline, battery, motors and driver model. Finally the parameters used for the vehicle model are discussed.

4.1. Vehicle model for tracking

The advised optimal speed profiles are often not tracked perfectly by the drivers [65], leading to a decrease in energy efficiency, an increase in travel time, and sometimes increase in speeds. Automated vehicle technologies help in reducing the tracking error of the optimal advised speed profiles. A longitudinal electric model is modelled in Simulink. The vehicle model is a standalone system and is independent of the controller. The output from the controller is fed to the vehicle model as input in terms of speed profiles [m/s]. The vehicle model is modelled to represent an automated vehicle that could track the optimal speed advice from the controller with minimized error in longitudinal velocity. Since the model is an battery electric vehicle (BEV), the state of charge (SoC) of the battery is considered as the fuel gauge as in a conventional internal combustion engine (ICE) vehicle. Thus it is necessary to calculate the SoC of the battery as an important parameter.

4.1.1. Assumptions

Various assumptions have been considered for modeling the BEV in this thesis. Since the controller designed in the Chapter 3 is a longitudinal controller, the vehicle model also concerns only the longitudinal dynamics (i.e) the acceleration and braking behaviour. The vehicle is assumed to travel on a flat smooth road without any grade or inclination. Since the application of the driving model relates to normal driving without any extreme handling maneuvers, the tires are considered to be linear in range. The rolling resistance of the vehicle is assumed to be constant with respect to changes in vehicle speed and tire pressure. Some losses due to friction and heat generation between components are neglected.

4.2. Vehicle subsystems

The model has various subsystems which are broadly categorised into two, the vehicle dynamics and powertrain systems respectively [71]. The powertrain subsystem consists of the electric motor, battery and the driveline. The vehicle dynamics subsystem consists of the

brakes, and the resistive forces. The chassis dynamics are modeled using relevant fundamental laws taking into account aerodynamic effects and road slope variation. The vehicle model with its subsystems is illustrated in figure 4.1

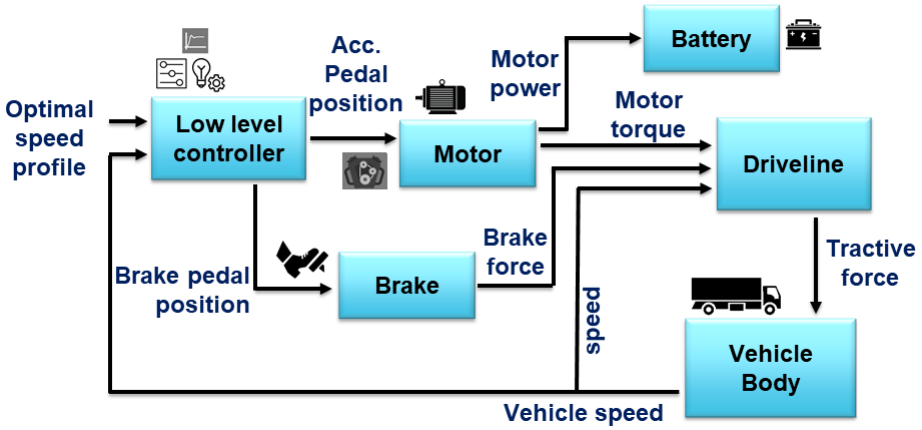

Figure 4.1. – Battery electric vehicle model with subsystems

4.2.1. Longitudinal dynamics system

The vehicle dynamics subsystem includes the longitudinal dynamics of the vehicle considering all the resistive forces from aerodynamics and gradient inclination. In order to make it more realistic, wheel dynamics is also included using the tire model.

Longitudinal Dynamics

The vehicle body is represented by a one degree-of-freedom (1DOF) model which accounts only for the longitudinal motion (forward and reverse motion). The longitudinal force in a vehicle consists of the longitudinal tire forces, aerodynamic drag forces, rolling resistance forces and gravitational forces [72]. The net tractive force of the vehicle is given by

$$F_{tr} = F_{aero} + F_i + F_{grade} + F_{rr} \tag{4.1}$$

where,
F_{tr} is the net longitudinal or tractive force of the vehicle
F_{aero} is the force due to aerodynamic drag
F_i is the inertial force of the vehicle
F_{grade} is the force due to gradient of the road
F_{rr} is the force due to rolling resistance.

The aerodynamic drag force (F_{aero}) of the vehicle is represented by the relation

$$F_{aero} = \frac{1}{2}\rho C_d A_f V^2 \tag{4.2}$$

where,
ρ is the air density in kg/m^3

C_d is co-efficient of aerodynamic drag
A_f is the frontal area of the vehicle in m^2
V is the longitudinal vehicle velocity in m/s

The force due to inertia of the vehicle is given by

$$F_i = m_i a \tag{4.3}$$

where,
m_i is the inertial mass of the vehicle in kg and is given by $1.04 * m$
a is the longitudinal acceleration of the vehicle in m/s^2.
The longitudinal acceleration of the vehicle is derived by substituting equation 4.3 in equation 4.1 as

$$a = \frac{F_{tr} - (F_{aero} + F_{grade} + F_{rr})}{m_i} \tag{4.4}$$

The gradient resistance force is mathematically represented as

$$F_{grade} = mgsin\theta \tag{4.5}$$

where,
m is the mass of the vehicle in kg
g is the acceleration due to gravity in m/s^2
θ is the angle of inclination of the road in $degrees$. Since the road considered for this research is flat and no inclination $\theta = 0$

The force due to rolling resistance is caused due to the friction between the wheels and the road when in contact. The equation for the rolling resistance force is given by

$$F_{rr} = mgC_{rr} \tag{4.6}$$

where,
C_{rr} is the co-efficient of rolling resistance.

This block in the model takes in the net tractive force from the tire model and outputs vehicle speed to the driver model.

4.2.2. Low level controller

The low level controller is a PID controller to track the error between the input optimal speed profile from the controller and the profile traced by the vehicle model. The PID output is normalized using the nominal velocity (lower range velocity) thus making it a command (no unit). The commands are further given a unit delay to mimic actuator delay and then the output signal is split into acceleration and braking commands. It is made sure that acceleration and braking commands don't overlap at the same time i.e only one pedal can be pressed at a time.

4.2.3. Brake system

This subsystem takes in the brake pedal position as the input from the low level controller and outputs brake force which is fed to the motor and driveline. The brake model is used to calculate the friction brake force F_b and the regenerative brake force F_{rb} using the brake pedal position from the low level controller.

$$F_b = B_{pos} \times F_{mbr} \times F_{brfrac} \tag{4.7}$$

$$F_{rb} = B_{pos} \times F_{mbr} \times R_{brfrac} \tag{4.8}$$

B_{pos} is the Brake Pedal Position. F_{mbr} is the maximum brake force of the vehicle. F_{brfrac} and R_{brfrac} are the friction brake fraction and regenerative brake fraction constants respectively. The regenerative braking is only activated when the vehicle speed is greater than 2m/s. This is to identify whether the vehicle is in motion.

4.2.4. Powertrain Dynamics

The powertrain dynamics mainly accounts for the motor, driveline, brakes. The battery is also included in the powertrain model for the estimation of the state of charge of the vehicle at realtime. The modelling of the powertrain is done with the help a of power loss approach [73]. The power loss model approach looks at the power flow through the vehicle and accounts for losses of each and every component associated. The power balance is through a component is given by

$$P_{out} = P_{in} - P_{loss} \times P_{in} \tag{4.9}$$

where P_{out} is the power output of the component, P_{in} is the power required for the component and P_{loss} is the losses associated with that component. The losses of the component can be expressed in terms of a second order polynomial such as

$$P_{loss} = C_0 + C_1 \times P_{in} + C_2^2 \times P_{in} \tag{4.10}$$

The first term is a constant accounting for windage loss and some magnetic loss, the second term is proportional to the output power accounting for frictional loss and some magnetic loss and a third part that is proportional to square of output power accounting for copper and battery losses. C_0, C_1 and C_2 are constant polynomial coefficients of power loss on the vehicle's component. Thus, this simple yet powerful approach is used for modelling the motor and battery.

4.2.5. Motor

The motor subsystem gets the accelerator pedal position from the low level controller, regenerative braking torque from the brake subsystem and motor speed ω as the inputs. The subsystem gives out motor power and motor torque as outputs to the battery and driveline.

The traction electric motor is modelled with the power loss approach motioned in the previous section. The power output P_{mout} is characterised by the mechanical output that comes from the shaft.

$$P_{mout} = T_{mot}\omega_{mot} \tag{4.11}$$

where T_{mot} is the torque of motor and ω_{mot} is the rotational speed of the motor. The losses in the motor are characterised with the help of the quadratic equation

$$P_{mloss} = K_c T_{mot}^2 + K_i \omega_{mot} + K_\omega \omega_{mot}^3 + C \tag{4.12}$$

The parameters such as K_c, K_i, K_ω, C correspond to the coefficients of various losses associated with the motor. Frictional and windage losses which depend on the motor speed and load torque, the magnetic loss which is dependent on the magnitude and frequency of supply voltage and copper loss in the motor are also included in the losses [73, 74]. The overall power required for the motor is given by the motor power input (P_{min})

$$P_{min} = P_{mout} + P_{mloss} \tag{4.13}$$

4.2.6. Battery

The motor power P_{mot} is given as input to the battery and it outputs the state of charge (SoC) of the battery. The battery modelling is done with the help of an internal resistance [75]. The auxiliary loads are also considered in the model. The battery model is a very simple model which does not consider battery chemistry for design simplification. The ideal power of the battery (P_{bideal}) is given by

$$P_{bideal} = I * V_{oc} \tag{4.14}$$

where I_b is the current in the battery and V_{oc} is the open circuit voltage of the battery. The ideal power can also be represented as

$$P_{bideal} = P_{bactual} + P_{bloss} \tag{4.15}$$

P_{actual} is the power at that time instance in the battery. The losses in the battery are due to the internal resistance R_{int} and the current associated with the battery.

$$P_{bloss} = I^2 R_{int} \tag{4.16}$$

The current in the battery is given expressed as

$$I = \frac{V_{oc} - \sqrt{V_{oc}^2 - 4R_{int}P_{bactual}}}{2R_{int}} \tag{4.17}$$

The voltage across the terminals of the battery V_{term} is given by

$$V_{term} = V_{oc} - IR_{int} \tag{4.18}$$

The state of charge SOC_{new} of the battery can also be calculated with the mathematical expression

$$SOC_{new} = SOC_{old} + 100\frac{dE_{int}}{E} \tag{4.19}$$

where SOC_{old} is the initial state of charge of the battery, dE_{int} is the change in internal energy of the battery and E is the total energy capacity of the battery.

4.2.7. Driveline system

The driveline model is used to transfer the output torque from the motor to the vehicle body. The model takes in the motor torque T_{mot}, Brake force F_b and vehicle speed V as the inputs and the tractive force F_{tr} and motor speed ω as the outputs. The tractive force can be obtained by the following equation

$$F_{tr} = (T_{mot} - T_{Dloss})\frac{G}{r_w} - F_b \tag{4.20}$$

$$T_{mot} = \frac{P_{mot.max}}{\omega} \tag{4.21}$$

where T_{Dloss} is the losses associated with the driveline which is mainly spin loss. The value of the spin loss is considered to be a constant. G is the overall gear ratio, r_w is the effective tire radius and F_b is the brake force of the vehicle. $P_{mot.max}$ is the maximum power output of the electric motor. The torque to the wheels or the wheel torque T_w is calculated with the help of relation [74]

$$F_w = \frac{T_w}{r_w} \tag{4.22}$$

$$T_w = \frac{G \times D_{final} \times T_{mot}}{2} \tag{4.23}$$

F_w is the force to the wheels or the net tractive force. G,D_{final} are the gearbox ratio and the final drive ratio respectively.

4.3. Vehicle model parameters

The parameters/coefficients used for modelling the electric vehicle model in Simulink environment is given in table 4.1 [75, 69]. The vehicle model is validated in the next chapter 5 though various drive cycles.

Table 4.1. – Parameters and coefficients for electric vehicle model

Notation	Parameter/coefficient	Value	Unit
m	Mass of the vehicle	1595	kg
ρ	Air density	1.23	kg/m^3
C_D	Aerodynamic drag coefficient	0.28	-
A_f	Frontal area of the vehicle	2.1	m^2
C_{rr}	Rolling resistance coefficient	0.01	-
m_i	Inertial mass of the vehicle	1658	kg
F_{mbr}	Maximum Brake Force	10000	N
R_{BF}	Regen Brake Fraction	0.55	-
r_w	Wheel radius	0.35	m
$T_{mot.max}$	Maximum motor torque	500	Nm
$P_{mot.max}$	Maximum motor power	100	kW
K_c	Motor loss coefficient	0.045	s/kg m^2
K_ω	Motor loss coefficient	5.066	kg/m^2
K_i	Motor loss coefficient	0.0166	J
C	Motor loss coefficient	628.2973	W
AL	Auxiliary load	700	W
V_{oc}	Open circuit voltage	340	V
R_{int}	Internal resistance	0.1	Ohm
T_{Dloss}	Driveline spin loss	6	Nm
G	Combined gear ratio	3.55	-
F_{mtr}	Maximum tractive force	5000	N
$Cap_{Battery}$	Energy capacity of battery	24	kWh
D_{final}	Final drive ratio	3.55	-
P	Proportional gain	2.5	-
I	Integral gain	2	-
D	Differential gain	0	-

5. Experimental Verification

This chapter presents the experiment and simulation results of the developed control algorithm. In section 5.1, different simulation scenarios with their settings and objectives are explained. Next, the scenarios in Section 5.2 used to validate the vehicle model and the tracking of controlled automated vehicle platoon are discussed. Finally, the performance indicator - energy consumption is addressed in Section 5.3.

5.1. Simulation scenarios

The performance of the controlled automated vehicle (CAV) platoon is analyzed using different scenarios. The number of vehicles in the controlled automated platoon is set to be $N = 10$ for the first three scenarios. The leader of the platoon starts from $L_0(200)$ meters away from the stop-line (0) meter in the intersection. The prediction horizon for the simulation is a sum of the green and red signal phase timings i.e; $T = g_i + r_i$. The cost weights for the objective function are tuned in the first baseline scenario and maintained the same for all the scenarios. Each scenario has a specific setting and objective as shown in table 5.1.

Table 5.1. – Simulation experiments

	Scenario design	Settings	Experiment objectives
Scenario 1	An isolated intersection without downstream queue	N = 10 g1 = 30 r1 = 30	To check the position constraints and extensibility of the control approach. To tune cost weights under eco-driving objective function
Scenario 2	An isolated intersection without downstream queue	N =10 g1 = 30 r1 = 30 g2 = 30	To check the effectiveness when the signal cycle is increased and verify the possible deceleration maneuvers.
Scenario 3	An arterial corridor with downstream queues (small and large) in signalized intersections	N = 10 Q = 3,9	To assess the application of controlled vehicles with a downstream queue, and position constraint for the leader vehicles
Scenario 4	Comparison of controlled automated vehicle platoon with IDM platoon	N = 5	To compare the performance of the controlled platoon with the IDM platoon
Scenario 5	Regenerative breaking analysis	N = 1	To study the regenerative effect of the equipped vehicles

5.1.1. Scenario 1: Baseline scenario - stopping at intersection

This scenario is designed in a way that the controlled automated vehicle platoon of 10 vehicles (N=*10*) splits into two parts at an isolated intersection without any downstream queue. One part of the platoon can pass through the intersection (q) at the present green phase (g_1) while the other part of the platoon (N-q) cannot pass through the intersection due to the red phase (r_1). The first green and red phase timings are set to be 30 seconds each. Thus, the prediction horizon (T) is 60 seconds, which is sum of the green phase (g_1) and red

phase ($r1$). The objective function for scenario 1 is formulated to minimize the travel delay and energy consumption for all the vehicles in the platoon within the prediction horizon. The cost weights of the eco-driving objective function is tuned with this baseline scenario as it optimizes the whole platoon. The cost weights for acceleration $\beta_1 = 0.5$ is set as the standard weight. Since, speed is linearly related to acceleration, the cost weight for speed term is same as that of acceleration $\beta_2 = 0.5$. The cost weight of energy consumption is set at $\beta_3 = 0.5$ and $\beta_4 = 0.5$, which does not contribute in any way as the term q in the objective function is a constant. The tuned cost weights are used for all the forthcoming scenarios. The simulated plots of acceleration, speed, position, and energy consumption of the controlled automated vehicle platoon for scenario 1 is shown in figure 5.1.

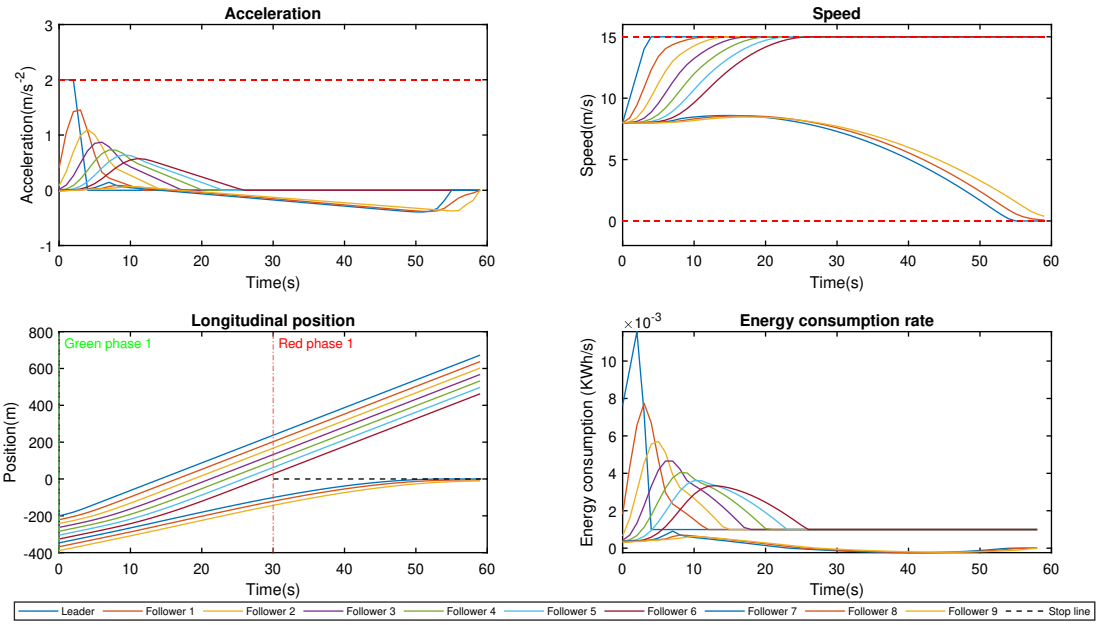

Figure 5.1. – Scenario 1: Baseline scenario

It can be seen from figure 5.1 that the first q=7 vehicles accelerate faster to reach the maximum speed limit v_{max} and then maintain the constant speed. The vehicles that cannot pass through the intersection N-q=3 vehicles, slowly decelerate and reach the stop line of the intersection in the red phase. This behavior of the vehicles that do not pass the intersection, is due to the energy consumption rate function in the optimization problem. It is also observed from the acceleration subplot that, only the first vehicle can achieve the maximum possible acceleration of $2m/s^2$, which is because the leader vehicle is not subjected to any safety constraints, unlike the following vehicles in the platoon. A significant reduction in energy consumption of vehicles *(N-q)* is also seen, which is due to the regenerative braking effect of the vehicles. This effect helps in charging the battery of those vehicles when decelerating towards the stop line.

5.1.2. Scenario 2: Extended signal cycle - Automated platoon at isolated intersection T = 90

For the second scenario, the signal phase cycle is increased by adding a second green phase g_2= 30 seconds to check the effectiveness of the platoon when the prediction horizon T is extended to 90 seconds. Like scenario 1, the controlled automated vehicle platoon consists of 10 vehicles (N=*10*) that are split at the isolated intersection. But unlike the scenario 1, the part of the platoon that could not pass the intersection, passes the intersection in the second green phase g_2 without stopping in the red phase at the stop line. The objective function for scenario 2 is formulated to minimize the travel delay of vehicles that pass the intersection at the first and second green phases g_1, g_2 and to minimize the energy consumption of the vehicles that could not pass through the intersection in the current green phase. The simulated plots for scenario 2 are shown in figure 5.2

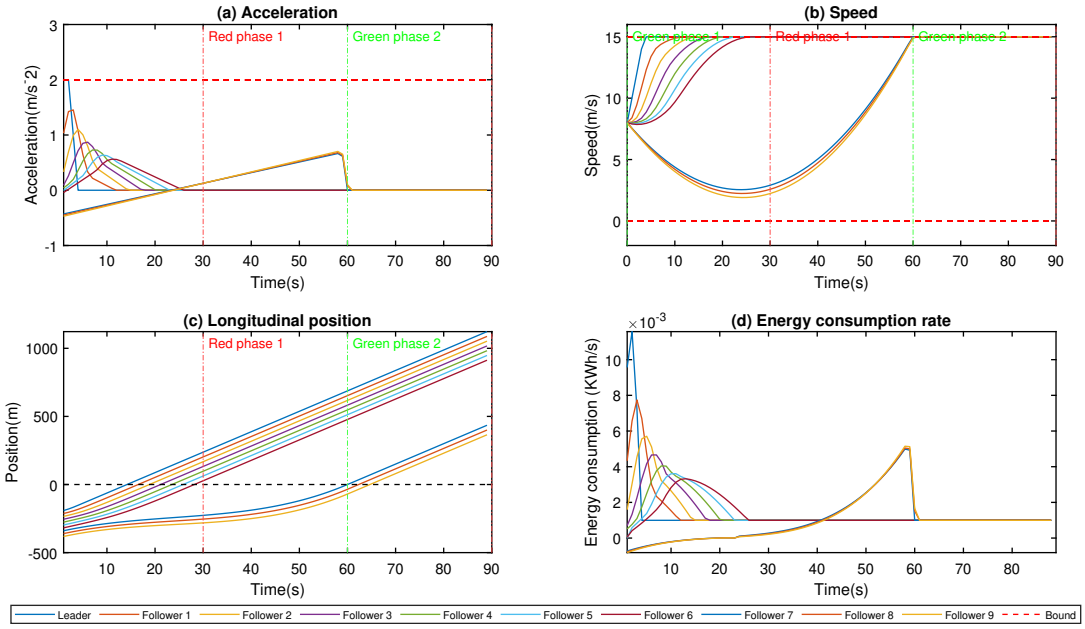

Figure 5.2. – Scenario 2: Automated platoon with extended signal cycle

As expected it can be seen in the longitudinal position subplot, that the N-q vehicles pass the intersection at the start of the second green phase g_2 and they do not come to rest in the red phase. The speed subplot shows that the vehicles that could not pass the intersection gradually decelerate in the current green phase g_1 and accelerates in the red phase r_1 to pass through the intersection at the second green phase g_2 with maximum speed v_{max}. After passing the intersection the vehicles maintain the constant maximum speed similar to the vehicles passing the intersection in the first green phase. Since the accelerations of all the vehicles in the platoon are controlled within the prediction horizon, the acceleration profiles are smooth and optimized as shown in the acceleration subplot. Energy consumption is directly influenced by acceleration and deceleration pattern of the platoon is also found to

be very low for vehicles that do not cross the intersection at the first green phase.

5.1.3. Scenario 3: Automated platoon at signalized intersection with downstream queue

In this scenario, the automated platoon performance is analyzed at a signalized intersection with a downstream queue. The queue is not controlled and is represented by the car-following model. The car-following model chosen in this thesis is the intelligent driver model (IDM) [76]. The modelling of the IDM platoon is described in Appendix C. Thus, the presence of an IDM queue in the intersection helps to create a mixed traffic environment of controlled and uncontrolled vehicles. The controlled automated vehicle platoon is simulated with smaller and larger queues at the intersection to assess the influence of the downstream queue. The introduction of queues also calls in for the collision avoidance constraint on the leader of the controlled vehicle platoon. The queue starts from rest at a position 0 or the stop line of the intersection, while the platoon leader is 200 m away from the stop line and traveling towards the intersection at a speed of $8m/s$.

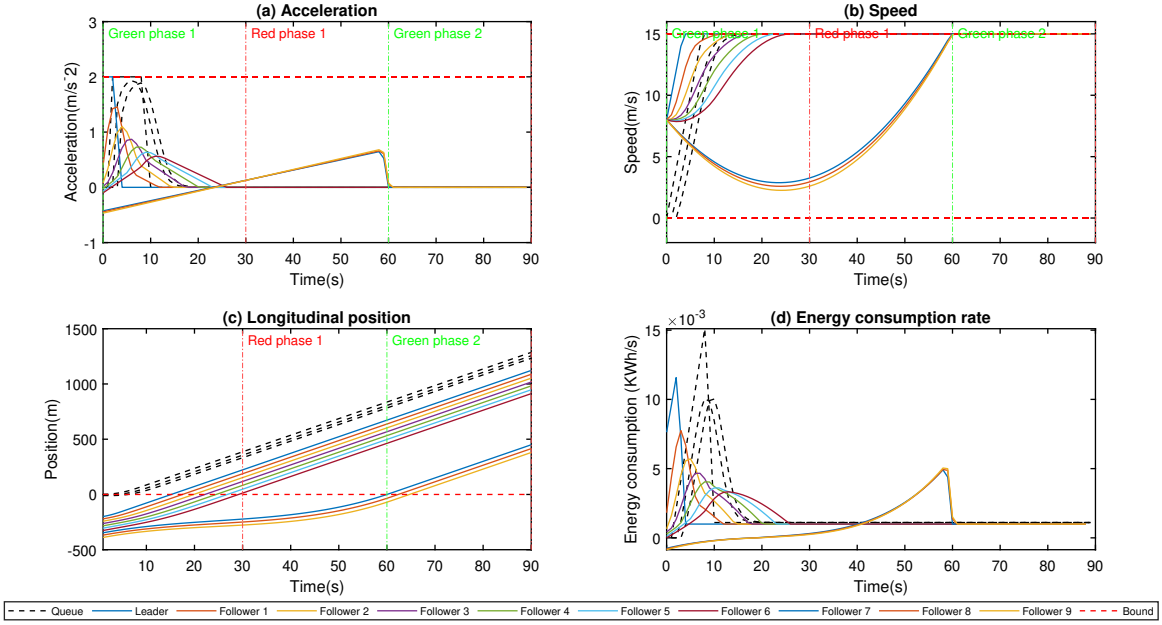

Figure 5.3. – Scenario 3: Controlled automated vehicle platoon with small queue at intersection

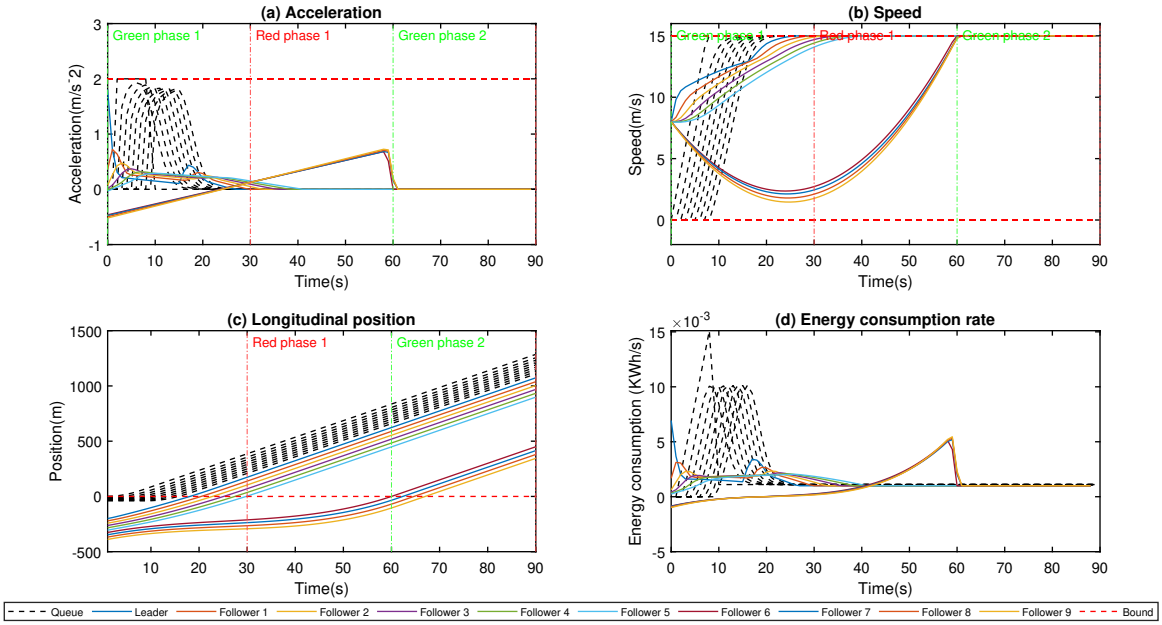

Figure 5.4. – Scenario 3: Controlled automated vehicle platoon with large queue at intersection

Initially, a small queue of Q=*3* vehicles is considered to be present at the signalized intersection during the first green phase g_1. The performance of the controlled automated vehicle platoon is not affected by a smaller queue as shown in figure 5.3. The IDM queue is represented using the black dotted lines. Figure 5.4 shows the performance of the controlled automated vehicle platoon under the influence of the larger queue Q=*9*. It can be observed that the number of vehicles in the downstream queue Q directly affects the number of controlled vehicles in the platoon passing the intersection. Thus, the number of controlled vehicles passing the intersection is reduced from q=*7 to* q=*6*. Since the leader is also constrained with collision avoidance (safety constraint), it accelerates until it comes in the region of a safe distance gap with the last vehicle in the IDM queue. Thus, it slows down to maintain the safe gap and then accelerates again to reach the maximum speed limit. This leads to the vehicles following in the controlled automated vehicle platoon to reach the maximum speed limit slightly later, when compared with the simulation with a smaller queue.

5.1.4. Scenario 4: Comparison of Automated platoon and IDM platoon

Current scenario is designed to compare the performance of the controlled automated vehicle platoon with the intelligent driver model platoon. Both the platoon is set to have 5 vehicles each *(N=5)*. Both platoons start from *0 m* position (stop line) and *0 m/s* initial speed simulated for a prediction horizon T=*90* seconds. All the vehicles in the platoon follow a minimum or desired safe time and space gap to avoid rear-end collisions throughout the simulation. The maximum speed limit for both the platoons was set to $v_{max} = 15m/s$. The simulation results of the IDM platoon are shown in figure 5.5 and the controlled automated vehicle platoon are shown in figure 5.6.

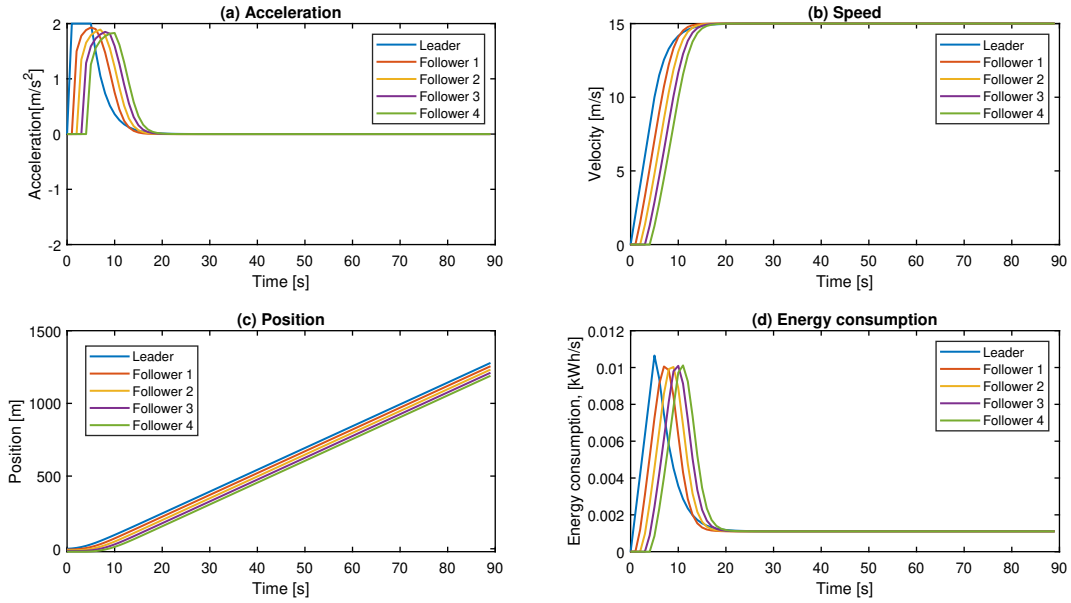

Figure 5.5. – Scenario 4: Human driven platoon/IDM platoon

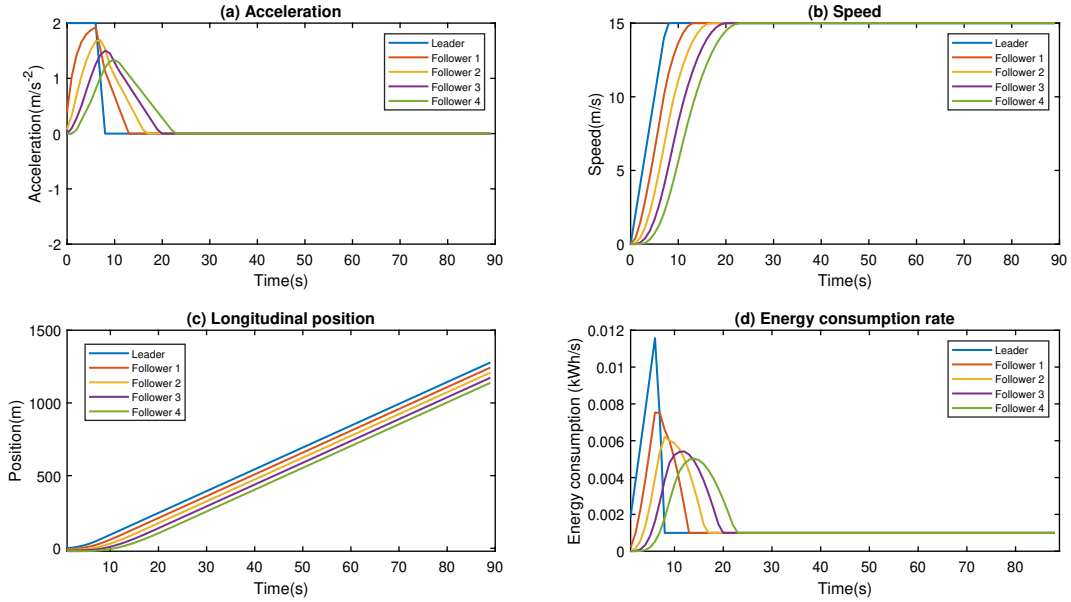

Figure 5.6. – Scenario 4: Controlled Automated Vehicle platoon

From the IDM platoon results, the figure 5.5 shows that the acceleration of followers is quite high when compared with the CAV platoon results in figure 5.6. This is due to the fact that the acceleration of the followers in the CAV platoon is optimized to a greater extent.

The followers in the IDM platoon accelerate at nearly the same values to reach the maximum speed limit, while the optimal values of acceleration of the followers in the CAV platoon are much lesser. The energy consumption rate of the CAV platoon was found to be lesser than the IDM platoon for the simulated scenario, which is a direct result of the acceleration and deceleration behavior of the platoon. The energy savings of the CAV platoon when compared with the IDM platoon is discussed later in section 5.3.1.

5.1.5. Scenario 5: Regenerative braking effect analysis

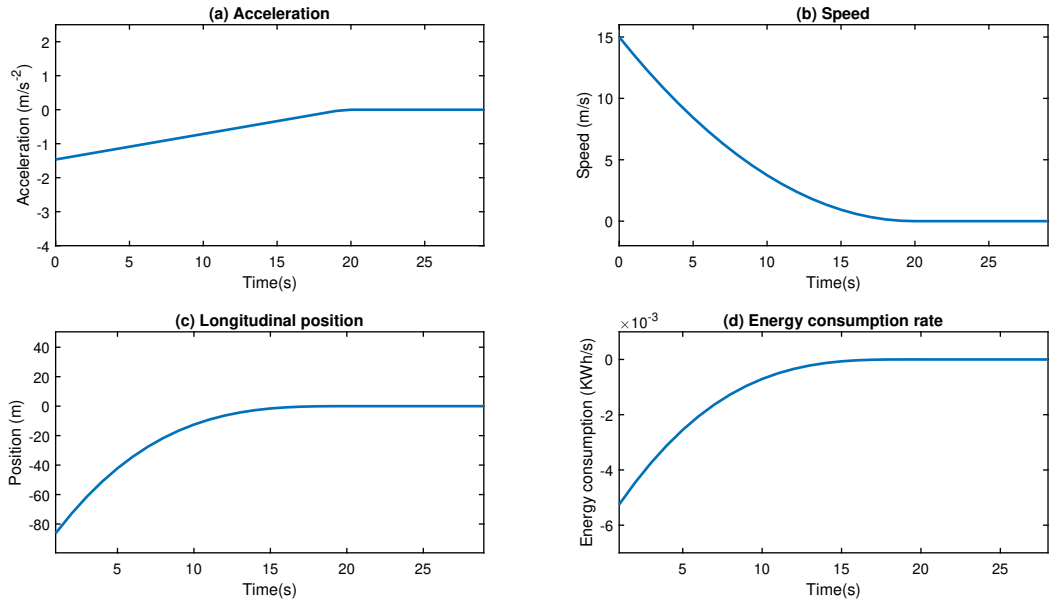

Figure 5.7. – Scenario 5: With regenerative braking

This scenario is simulated to study the effect of regenerative braking for the equipped vehicles and their significance. In order to understand the effect one controlled vehicle is set to start from a position of 100 m away from the intersection stop line and with 15 m/s initial speed which is the maximum allowable speed. The vehicle is simulated to start with the maximum speed and gradually decelerated to rest position in front of the stop line. The experiment was simulated for time of 30s corresponding to a green phase. In order to understand the braking effect much better, the simulation was repeated for a vehicle with regenerative braking and the results were compared. The simulation results for vehicle equipped with and without the regenerative braking are shown in figure 5.7 and figure 5.8 respectively.

From figure 5.7, it can be seen that, when the vehicle starts to decelerate it results in negative acceleration leading to regenerative braking effect. During this phase, the equipped vehicle regenerates energy by allowing the motor to rotate in opposite direction and recharge the battery. Thus, resulting in negative energy consumption. But, it can be seen from the

figure 5.8 showing the behaviour of vehicle without regenerative braking that it does not regenerate any energy during the same course of action. It consumes only the auxiliary power $P_{Auxiliary} = 5.389 \times e^{-10}$ during braking and zero acceleration. It is also observed that the vehicles equipped with regenerative braking had slightly optimized values of acceleration when compared with unequipped vehicles.

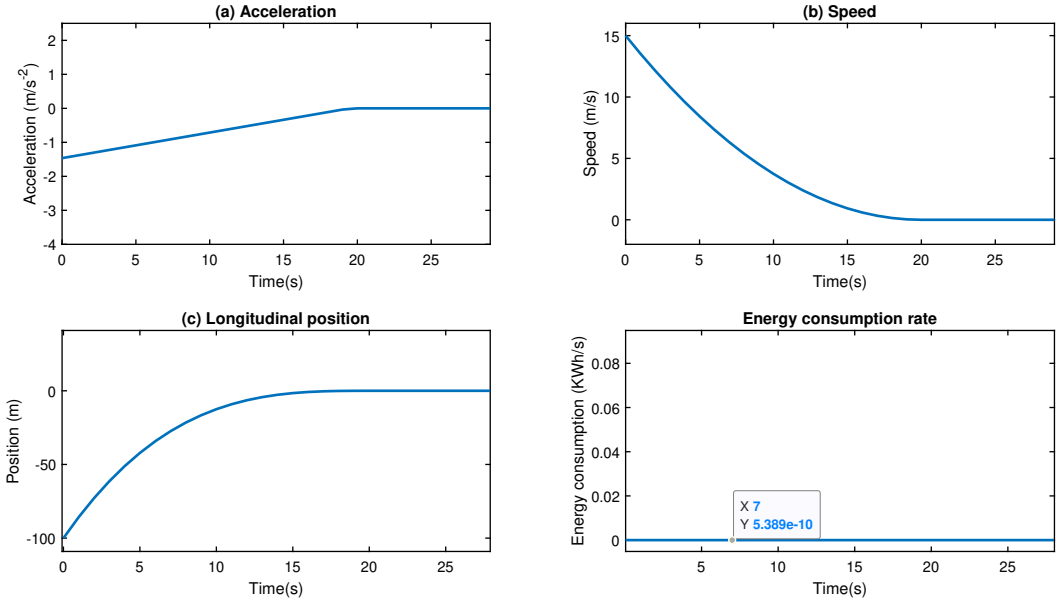

Figure 5.8. – Scenario 5: Without regenerative braking

5.2. Vehicle model validation

The vehicle model developed in chapter 4 is validated in this section, using different drive cycles like the New European Driving Cycle (NEDC) and the Urban Dynamometer Driving Schedule (UDDS). The drive cycles were selected based on the application of control algorithm which is designed for urban scenarios. The NEDC represents the driving behaviour in Europe, which consists of four repeated ECE-15 urban driving cycles (UDC) and one Extra Urban Driving Cycle (EUDC). The UDDS is used to represent the city driving conditions, also known as the Federal Test Procedure (FTP) cycle. Both drive cycles are used to estimate fuel/energy consumption and emission of vehicles. The main characteristics of both drive cycles are given in the table 5.2. Since the thesis deals with electric vehicles, the state of charge of the battery is also measured for the following drive cycles.

Table 5.2. – Drive cycle characteristics

Drive cycle	Distance [m]	Duration [s]	Average speed [m/s]	Max speed [m/s]
NEDC	11023	1180	9.33	35
UDDS	12070	1369	8.75	25

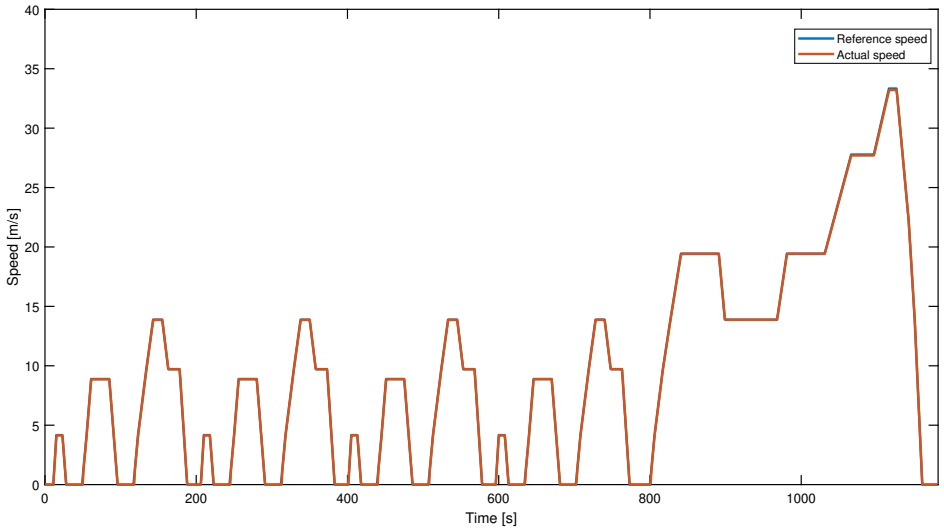

Figure 5.9. – Tracking of NEDC drive cycle

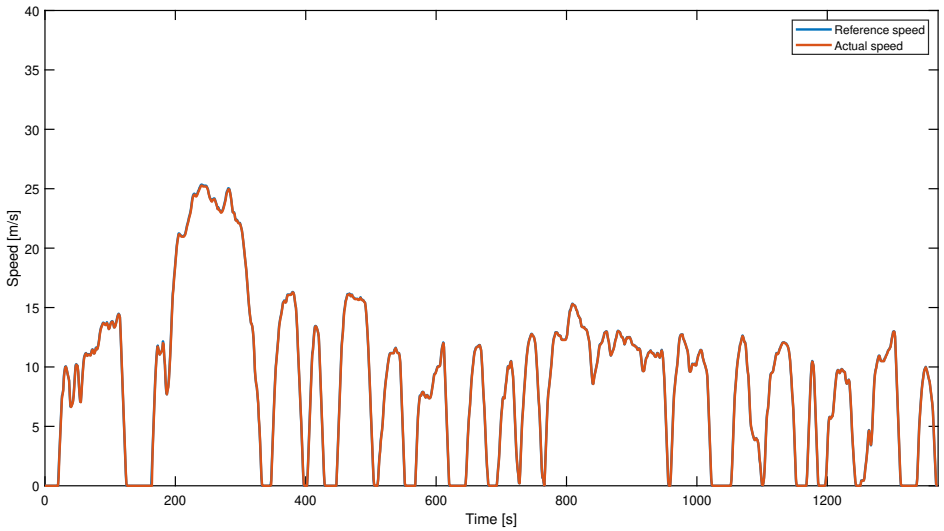

Figure 5.10. – Tracking of UDDS drive cycle

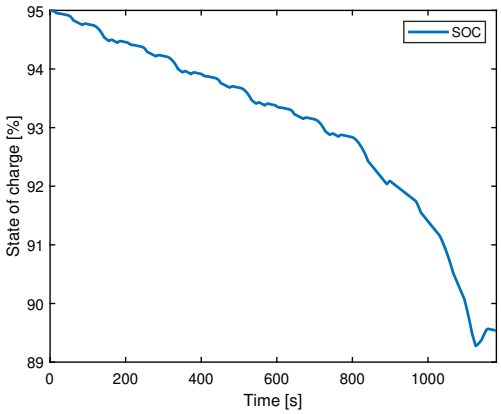

Figure 5.11. – SOC of NEDC drive cycle

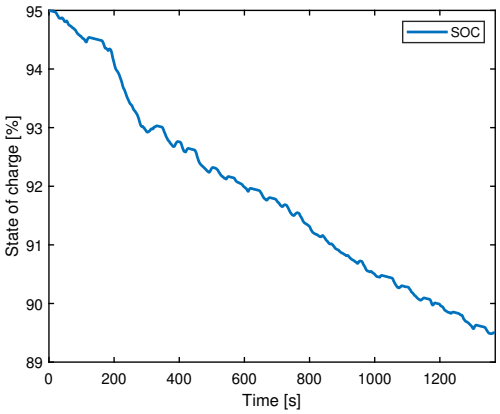

Figure 5.12. – SOC of UDDS drive cycle

Speed profiles of the NEDC and UDDS drive cycles are tracked using the developed vehicle model. The vehicle model was able to track the drive cycles quite comfortably as shown in figures 5.9 and 5.10. The red curve shows the vehicle tracking and the blue curve represents the reference speed of the drive cycle. The root mean square error between the reference and actual values is found to be 0.01. The plots for SOC of both the drive cycles are shown in figure 5.11 and 5.12. The peaks and bumps in the plot are due to the increase in state of charge, as a result of regenerative braking effect during deceleration of the electric vehicle.

5.2.1. Tracking of automated platoon using vehicle model

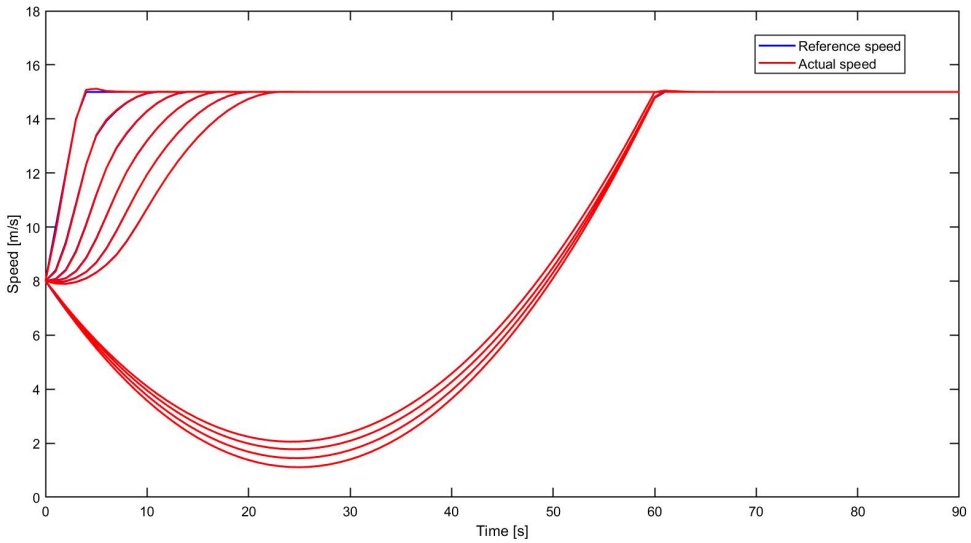

Figure 5.13. – Tracking using vehicle model

The main outputs of the developed longitudinal electric vehicle model are to track the longitudinal velocity and to find the SOC of the battery. To track the longitudinal velocity of the controlled automated platoon, the simulation scenario 2 from section 5.1.2 is selected. The CAV platoon starts from a distance of 200 meters away from the stop line of the intersection. The whole platoon has an initial speed of $8m/s$ at the start of the simulation. The simulation is carried out for a prediction horizon of $T = 90$ seconds. The output of the control algorithm is the optimal speed profile of the CAV platoon in the vicinity of a signalized intersection. The optimal speed profile is tracked using the longitudinal electric vehicle model with the help of a closed-loop PID controller as discussed in chapter 4. The tracking of the CAV platoon is shown in figure 5.13, the blue curves in the plot correspond to the optimal speed profile of the CAV platoon from the control algorithm, while the red curves show the curves traced by the vehicle model platoon. It was found that the root mean square error in tracking was only 1%. This shows that the developed vehicle model is capable of tracking the optimal speed profile from the control algorithm without any discomfort. Thus the application of automated vehicles in eco-driving can be used to overcome the inability of the human driver to track the optimal speed profile as advised by eco-driving technologies.

5.2.2. State of charge evaluation

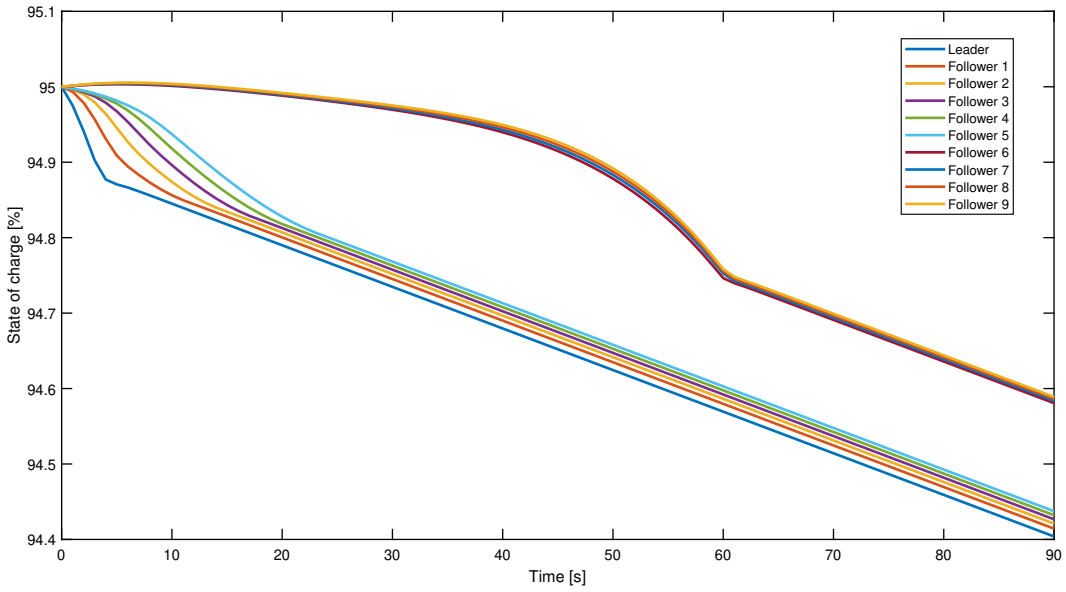

Figure 5.14. – SoC curves of the automated platoon

The state of charge for the tracked scenario is also calculated as shown in figure 5.14. The initial state of charge of the battery when fully charged is assumed to be 95%. The state of charge of the battery is directly associated with the change in internal energy of the battery and battery capacity as explained in section 4.2.6. From figure 5.14, it can be seen that the state of charge for the first seven vehicles (leader - follower 6) which pass the intersection

at the first green phase decreases rapidly, which is due to the vehicles accelerating faster to reach the maximum speed limit. Once the vehicles reach the maximum velocity and maintain the constant speed, it can be seen that the SOC of the vehicles decreases steadily. The other three vehicles (follower 7 - follower 10) which cannot pass the intersection at green phase starts to decelerate. When the vehicles decelerate, the electric power in the motor becomes negative. During this phase, energy flows from the wheels to the motor; the energy from the motor is used to charge the batteries, which leads to increase in SOC of the vehicles during this phase. The SOC starts to drop once the vehicles start to accelerate to reach the stop line of the intersection, and decreases steadily after the vehicles reach a constant speed.

5.3. Performance indicators

To assess and compare the performance of the developed CAV platoon the key performance indicators are defined.

5.3.1. Energy consumption/km

Energy efficiency is selected as a key performance parameter as it is one of the main parameters optimized using the developed algorithm. Energy cosumption per km is measured to compare the performance of the CAV platoon and the IDM platoon. The energy consumption/km of both platoons from simulation scenario 4 as in section 5.1.4 is calculated as shown in Figure 5.15 and 5.16. The energy consumption/km of IDM platoon was estimated to be 0.2839 kWh/km and 0.09221 kWh/km for CAV platoon. Energy consumption/km of the CAV platoon is 67% lesser than the energy consumption of IDM platoon for the simulated scenario as illustrated in figure 5.17. According to Allego, a charging solutions company, electric vehicle charging in Europe is priced at 0.22 cents per kWh [77]. Thus the cost of energy consumption/km for the CAV platoon is calculated to be 0.0202 euros/km and 0.062 euros/km for the IDM platoon.

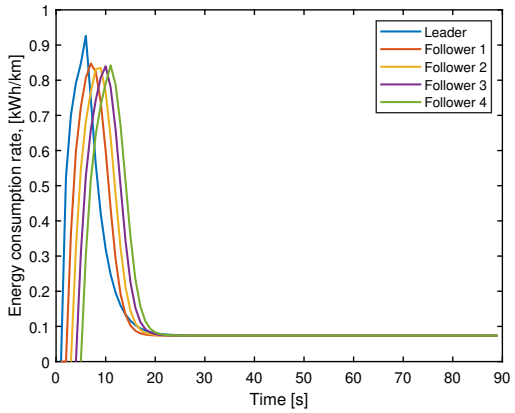

Figure 5.15. – Energy consumption per km of IDM platoon

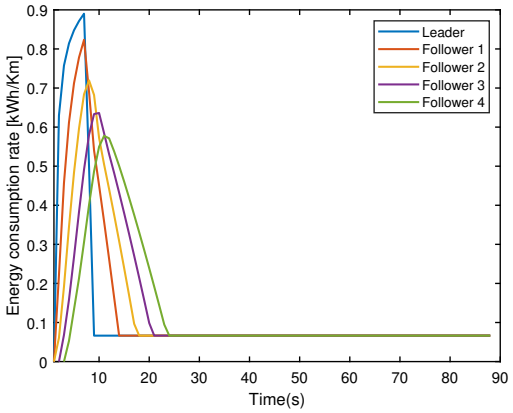

Figure 5.16. – Energy consumption per km of Automated platoon

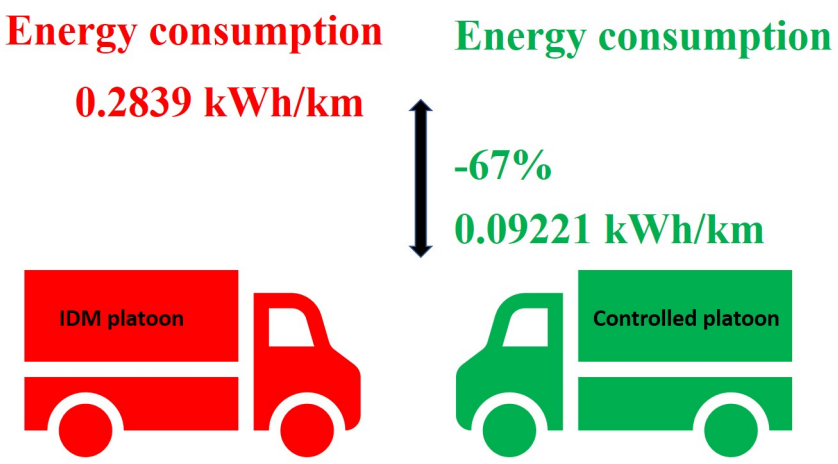

Figure 5.17. – Energy consumption savings of CAV platoon

5.4. Summary

In this chapter various scenarios were simulated to test the performance of the automated platoon and the results were observed. The first scenario is a basic scenario where the vehicles were just simulated for one signal cycle. In this scenario the the allowed vehicles pass through the intersection in the current green phase while the remaining vehicles come to a halt before the intersection. This scenario was simulated to check the working of the position constraints and cost weights of the control algorithm. In the second scenario the same platoon is simulated for a extended signal cycle, where the vehicles that could not pass the intersection in the current remaining green phase of the first scenario are allowed to pass the intersection in the second green phase with maximum speeds. This scenario shows the adaptability of the control algorithm to work for larger signal cycles. In the third scenario, the working of the algorithm with a queue in the intersection was checked. Both small and large queues were simulated and it was found that larger queues had significant effects in the performance of the platoon. This scenario was also used to test collision constraint for the leader in the vicinity of a queue. The fourth scenario compares the performance of the automated platoon with the IDM platoon, resulting in positive and better performance of the automated platoon in terms of optimized acceleration and energy consumption. Finally the effect of regenerative braking was shown in scenario five, where one vehicle was simulated with and without regenerative braking. It was found that the vehicle with regenerative braking effect generated energy while braking leading to lesser energy consumption than the vehicle without regenerative braking.

6. Conclusions and recommendations

This chapter provides the conclusion of the thesis in section 6.1 and the recommendations for future research in section 6.2.

6.1. Conclusions

The main objective of this research was to design an energy efficient longitudinal controller for electric vehicle platoons at signalized intersections. The research was split into several phases to fulfil the objective. First, a detailed literature study was performed. The literature study gave insights into state-of-the-art longitudinal control technologies for connected and automated vehicles. The study also helped in understanding the various state-of-the-art instantaneous energy consumption rate estimation models used for predicting and calculating the energy usage and savings of EVs. With the insights from the literature, a longitudinal controller was then designed using the optimal control method. The controller was modelled with the help of system dynamics, cost functions of different scenarios and constraints. The optimal controller was also tuned to achieve the desired performance. Further, various scenarios were designed to achieve the research goal and to assess the performance of the controller. A battery electric vehicle was modelled in Simulink, and was used to track the optimal speed profile from the optimal controller. Finally, the designed scenarios were simulated and performance indicators were identified.

From the literature study, it was concluded that energy consumption optimization requires an accurate energy consumption model. Thus VT-CPEM model was chosen, since it is a simple and an efficient model used for estimating the instantaneous energy consumption of EVs. Also, it captures the regenerative braking realistically by considering it as a function of deceleration. The model was validated by various drive cycles and compared with the actual model. Various optimal control strategies were also explored and their merits and shortcomings were studied.

The longitudinal controller for the platoon was modelled with the help of an optimal control problem. A nonlinear objective function was defined and constrained with linear equality and inequality constraints. The defined optimal control problem was solved using a direct optimal control method (i.e) transforming it to a nonlinear programming problem. The nonlinear programming problem was solved in CasADi (integrated with MATLAB interface) which is an open source tool for nonlinear optimization.

The thesis also includes a battery electric vehicle model designed in Simulink. The purpose of the model is to show that an autonomous vehicle will be able to track the optimal speed profile from the optimal controller. The optimal controller acts as the high-level controller while the PID in the vehicle model acts as the low level controller. The low level controller is

used to track the error between the speed profiles from the controller and the vehicle model. The vehicle model consists of an electric motor, battery and driveline system. One of the outputs of the model is the SoC of vehicle's battery.

It was found from the simulations that the controller was able to minimize the energy consumption and travel delay of the vehicles simultaneously. The results also show that the platoon maintains comfortable accelerations at all time. Rear end collisions are also avoided by constraining the vehicles with a safe gap. The controller also performs efficiently in the presence of queues (short or longer queues) in the upstream intersection. Finally it was concluded that when compared with the IDM platoon of same characteristics as the automated platoon, the controlled automated vehicle platoon reduces energy consumption and cost by 67% for scenario 4. Also, the vehicle model was able to track the optimal speed profile from the optimal controller with a RMSE error of 1%.

6.2. Recommendations

In this section, recommendations for future research are discussed. The research performed is only for a single intersection. This can be extended to corridor of intersections. This can be done by adding changes to the cost function. It will also be interesting to simulate a mixed vehicle environment as this work is assumed to be a fully automated environment. This might help in studying the performance of the controller with other vehicles around. The formation of the platoon is not addressed in this work, it was considered that the vehicles are already in a platoon. Thus, modelling the formation and merging of the platoon would be very useful. The controller implemented in this thesis is a optimal controller without feedback; thus solving the problem with model predictive control (MPC) method could yield better results. The vehicle model can also be included inside the closed loop with MPC method. The controller is computationally fast, however the computational time increases with the number of variables. Tuning the controller for real time purposes can be tedious and needs improvement. The traffic cycle implemented in the simulation consists only of the green and red phase, inorder to make it more realistic, a yellow phase can be introduced which might bring in changes in the platoon response. Further the research can also be extended by adaptive signal timings which might result in further optimization of travel time and energy consumption rate of the platoons.

Bibliography

[1] Alberto Bull, NU CEPAL, et al. *Traffic Congestion: The Problem and how to Deal with it*. ECLAC, 2003.

[2] Franke, F. Bottiger, Z. Zomotor, and D. Seeberger. Truck platooning in mixed traffic. In *Proceedings of the Intelligent Vehicles '95. Symposium*, pages 1–6, Sep. 1995.

[3] Robbert Janssen, Han Zwijnenberg, Iris Blankers, and Janiek de Kruijff. Truck platooning. *Driving the future*, 2015.

[4] Apoorva Saxena, Hong Li, Dip Goswami, and Chetan Belagal Math. Design and analysis of control strategies for vehicle platooning. In *2016 IEEE 19th International Conference on Intelligent Transportation Systems (ITSC)*, pages 1805–1812. IEEE, 2016.

[5] X. Qi, G. Wu, P. Hao, K. Boriboonsomsin, and M. J. Barth. Integrated-connected eco-driving system for phevs with co-optimization of vehicle dynamics and powertrain operations. *IEEE Transactions on Intelligent Vehicles*, 2(1):2–13, 2017.

[6] Peng Chen, Cong Yan, Jian Sun, Yunpeng Wang, Shenyang Chen, and Keping Li. Dynamic eco-driving speed guidance at signalized intersections: Multivehicle driving simulator based experimental study. *Journal of Advanced Transportation*, 2018, 2018.

[7] Hao Yang, Fawaz Almutairi, and Hesham A Rakha. Eco-driving at signalized intersections: A multiple signal optimization approach. *arXiv preprint arXiv:2001.01117*, 2020.

[8] Weiming Zhao, Dong Ngoduy, Simon Shepherd, Ronghui Liu, and Markos Papageorgiou. A platoon based cooperative eco-driving model for mixed automated and human-driven vehicles at a signalised intersection. *Transportation Research Part C: Emerging Technologies*, 95:802–821, 2018.

[9] Erik Hellström, Maria Ivarsson, Lars Nielsen, et al. Look-ahead control for heavy trucks to minimize trip time and fuel consumption. *IFAC Proceedings Volumes*, 40(10):439–446, 2007.

[10] Frank Lattemann, Konstantin Neiss, Stephan Terwen, and Thomas Connolly. The predictive cruise control–a system to reduce fuel consumption of heavy duty trucks. *SAE transactions*, pages 139–146, 2004.

[11] Behrang Asadi and Ardalan Vahidi. Predictive cruise control: Utilizing upcoming traffic signal information for improving fuel economy and reducing trip time. *IEEE transactions on control systems technology*, 19(3):707–714, 2010.

[12] Thijs Van Keulen, Gerrit Naus, Bram De Jager, René Van De Molengraft, Maarten Steinbuch, and Edo Aneke. Predictive cruise control in hybrid electric vehicles. *World Electric Vehicle Journal*, 3(3):494–504, 2009.

[13] Lior Simchon and Raul Rabinovici. Real-Time Implementation of Green Light Optimal Speed Advisory for Electric Vehicles. *Vehicles*, 2(1):35–54, 2020.

[14] M. Sanchez, J. Cano, and D. Kim. Predicting traffic lights to improve urban traffic fuel consumption. In *2006 6th International Conference on ITS Telecommunications*, pages 331–336, 2006.

[15] K. Katsaros, R. Kernchen, M. Dianati, and D. Rieck. Performance study of a green light optimized speed advisory (glosa) application using an integrated cooperative its simulation platform. In *2011 7th International Wireless Communications and Mobile Computing Conference*, pages 918–923, 2011.

[16] Marcin Seredynski, Bernabe Dorronsoro, and Djamel Khadraoui. Comparison of Green Light Optimal Speed Advisory approaches. *IEEE Conference on Intelligent Transportation Systems, Proceedings, ITSC*, (October 2017):2187–2192, 2013.

[17] Folko Flehmig, Amir Sardari, Uta Fischer, and Andreas Wagner. Energy optimal adaptive cruise control during following of other vehicles. In *2015 IEEE Intelligent Vehicles Symposium (IV)*, pages 724–729. IEEE, 2015.

[18] Folko Flehmig, Amir Sardari, Uta Fischer, and Andreas Wagner. Energy optimal adaptive cruise control during following of other vehicles. In *2015 IEEE Intelligent Vehicles Symposium (IV)*, pages 724–729. IEEE, 2015.

[19] Stefan Koehler, Alexander Viehl, Oliver Bringmann, and Wolfgang Rosenstiel. Improved energy efficiency and vehicle dynamics for battery electric vehicles through torque vectoring control. In *2015 IEEE Intelligent Vehicles Symposium (IV)*, pages 749–754. IEEE, 2015.

[20] Emily Pindilli. Applications for the environment: Real-time information synthesis (aeris)âbenefit-cost analysis. *Federal Highway Administration Office, US Department of Transportation: Washington, DC, USA*, 2012.

[21] Pantelis Kopelias, Elissavet Demiridi, Konstantinos Vogiatzis, Alexandros Skabardonis, and Vassiliki Zafiropoulou. Connected & autonomous vehicles–environmental impacts–a review. *Science of The Total Environment*, 712:135237, 2020.

[22] Hao Yang, Hesham Rakha, and Mani Venkat Ala. Eco-cooperative adaptive cruise control at signalized intersections considering queue effects. *IEEE Transactions on Intelligent Transportation Systems*, 18(6):1575–1585, 2016.

[23] X. Qi, P. Wang, G. Wu, K. Boriboonsomsin, and M. J. Barth. Energy and mobility benefits from connected ecodriving for electric vehicles. In *2017 IEEE 20th International Conference on Intelligent Transportation Systems (ITSC)*, pages 1–6, 2017.

[24] Xiaozheng He, Henry X Liu, and Xiaobo Liu. Optimal vehicle speed trajectory on a signalized arterial with consideration of queue. *Transportation Research Part C: Emerging Technologies*, 61:106–120, 2015.

[25] Haitao Xia, Guoyuan Wu, Kanok Boriboonsomsin, and Matthew J Barth. Development and evaluation of an enhanced eco-approach traffic signal application for connected vehicles. In *16th International IEEE Conference on Intelligent Transportation Systems (ITSC 2013)*, pages 296–301. IEEE, 2013.

[26] Peng Hao, Guoyuan Wu, Kanok Boriboonsomsin, and Matthew J Barth. Eco-approach and departure (ead) application for actuated signals in real-world traffic. *IEEE Transactions on Intelligent Transportation Systems*, 20(1):30–40, 2018.

[27] Simon Stebbins, Mark Hickman, Jiwon Kim, and Hai L Vu. Characterising green light optimal speed advisory trajectories for platoon-based optimisation. *Transportation Research Part C: Emerging Technologies*, 82:43–62, 2017.

[28] Hesham Rakha and Raj Kishore Kamalanathsharma. Eco-driving at signalized intersections using v2i communication. In *2011 14th international IEEE conference on intelligent transportation systems (ITSC)*, pages 341–346. IEEE, 2011.

[29] Raj Kishore Kamalanathsharma, Hesham A Rakha, and Hao Yang. Networkwide impacts of vehicle ecospeed control in the vicinity of traffic signalized intersections. *Transportation Research Record*, 2503(1):91–99, 2015.

[30] Hao Yang, Hesham Rakha, and Mani Venkat Ala. Eco-cooperative adaptive cruise control at signalized intersections considering queue effects. *IEEE Transactions on Intelligent Transportation Systems*, 18(6):1575–1585, 2016.

[31] Ronald T van Katwijk and Sabine Gabriel. Optimising a vehicle's approach towards an adaptively controlled intersection. *IET Intelligent Transport Systems*, 9(5):479–487, 2015.

[32] Gerard Aguilar Ubiergo. Mobility and environment improvement of signalized networks through vehicle-to-infrastructure (v2i) communications. B.S. thesis, Universitat Politècnica de Catalunya, 2013.

[33] Behrang Asadi and Ardalan Vahidi. Predictive cruise control: Utilizing upcoming traffic signal information for improving fuel economy and reducing trip time. *IEEE transactions on control systems technology*, 19(3):707–714, 2010.

[34] Md Abdus Samad Kamal, Masakazu Mukai, Junichi Murata, and Taketoshi Kawabe. Model predictive control of vehicles on urban roads for improved fuel economy. *IEEE Transactions on control systems technology*, 21(3):831–841, 2012.

[35] Jack Macki and Aaron Strauss. *Introduction to optimal control theory*. Springer Science & Business Media, 2012.

[36] Raj Kishore Kamalanathsharma and Hesham A. Rakha. Multi-stage dynamic programming algorithm for eco-speed control at traffic signalized intersections. *IEEE Conference on Intelligent Transportation Systems, Proceedings, ITSC*, (Itsc):2094–2099, 2013.

[37] Giovanni De Nunzio, Carlos Canudas de Wit, Philippe Moulin, and Domenico Di. Eco-driving in urban traffic networks using traffic signals information. *International Journal of Robust and Nonlinear Control*, (October 2015):23, 2015.

[38] Huifu Jiang, Jia Hu, Shi An, Meng Wang, and Byungkyu Brian Park. Eco approaching at an isolated signalized intersection under partially connected and automated vehicles environment. *Transportation Research Part C: Emerging Technologies*, 79:290–307, 2017.

[39] Meiqi Liu, Meng Wang, and Serge Hoogendoorn. Optimal platoon trajectory planning approach at arterials. *Transportation Research Record*, 2673(9):214–226, 2019.

[40] Xuewei Qi, Guoyuan Wu, Kanok Boriboonsomsin, and Matthew J. Barth. Data-driven decomposition analysis and estimation of link-level electric vehicle energy consumption under real-world traffic conditions. *Transportation Research Part D: Transport and Environment*, 64(April 2017):36–52, 2018.

[41] Ziran Wang, Guoyuan Wu, Peng Hao, and Matthew J. Barth. Cluster-Wise Cooperative Eco-Approach and Departure Application for Connected and Automated Vehicles Along Signalized Arterials. *IEEE Transactions on Intelligent Vehicles*, 3(4):404–413, 2018.

[42] Osman D. Altan, Guoyuan Wu, Matthew J. Barth, Kanok Boriboonsomsin, and John A. Stark. GlidePath: Eco-Friendly Automated Approach and Departure at Signalized Intersections. *IEEE Transactions on Intelligent Vehicles*, 2(4):266–277, 2017.

[43] Osman D. Altan, Guoyuan Wu, Matthew J. Barth, Kanok Boriboonsomsin, and John A. Stark. GlidePath: Eco-Friendly Automated Approach and Departure at Signalized Intersections. *IEEE Transactions on Intelligent Vehicles*, 2(4):266–277, 2017.

[44] Baisravan HomChaudhuri, Ardalan Vahidi, and Pierluigi Pisu. A fuel economic model predictive control strategy for a group of connected vehicles in urban roads. *Proceedings of the American Control Conference*, 2015-July:2741–2746, 2015.

[45] Aleksandar Stevanovic, Jelka Stevanovic, and Cameron Kergaye. Green light optimized speed advisory systems. *Transportation Research Record*, (2390):53–59, 2013.

[46] Fei Ye, Peng Hao, Xuewei Qi, Guoyuan Wu, Kanok Boriboonsomsin, and Matthew Barth. Prediction-based eco-approach and departure strategy in congested urban traffic. 2017.

[47] Guoyuan Wu, Fei Ye, Peng Hao, Danial Esaid, Kanok Boriboonsomsin, and Matthew J Barth. Deep learning–based eco-driving system for battery electric vehicles. 2019.

[48] Peng Hao, Zhensong Wei, Zhengwei Bai, and Matthew J Barth. Developing an adaptive strategy for connected eco-driving under uncertain traffic and signal conditions. 2020.

[49] Thomas Kirschstein and Frank Meisel. Ghg-emission models for assessing the eco-friendliness of road and rail freight transports. *Transportation Research Part B: Methodological*, 73:13–33, 2015.

[50] Rui Zhang and Enjian Yao. Mesoscopic model framework for estimating electric vehiclesâ energy consumption. *Sustainable Cities and Society*, 47:101478, 2019.

[51] Ganesh Mohan, Francis Assadian, and Stefano Longo. Comparative analysis of forward-facing models vs backward-facing models in powertrain component sizing. 2013.

[52] Tony Markel, Aaron Brooker, T Hendricks, V Johnson, Kenneth Kelly, Bill Kramer, Michael OâKeefe, Sam Sprik, and Keith Wipke. Advisor: a systems analysis tool for advanced vehicle modeling. *Journal of power sources*, 110(2):255–266, 2002.

[53] Chiara Fiori, Kyoungho Ahn, and Hesham A. Rakha. Power-based electric vehicle energy consumption model: Model development and validation. *Applied Energy*, 168:257–268, 2016.

[54] Teemu Halmeaho, Pekka Rahkola, Ari Pekka Pellikka, Kari Tammi, and Sami Ruotsalainen. Electric City Bus Energy Flow Model and Its Validation by Dynamometer Test. *2015 IEEE Vehicle Power and Propulsion Conference, VPPC 2015 - Proceedings*, pages 1–6, 2015.

[55] Chiara Fiori, Kyoungho Ahn, and Hesham A. Rakha. Microscopic series plug-in hybrid electric vehicle energy consumption model: Model development and validation. *Transportation Research Part D: Transport and Environment*, 63(May):175–185, 2018.

[56] Rui Zhang and Enjian Yao. Electric vehicles' energy consumption estimation with real driving condition data. *Transportation Research Part D: Transport and Environment*, 41:177–187, 2015.

[57] Shichun Yang, Cheng Deng, Tieqiao Tang, and Yongsheng Qian. Electric vehicle's energy consumption of car-following models. *Nonlinear Dynamics*, 71(1-2):323–329, 2013.

[58] Xinkai Wu, Xiaozheng He, Guizhen Yu, Arek Harmandayan, and Yunpeng Wang. Energy-Optimal Speed Control for Electric Vehicles on Signalized Arterials. *IEEE Transactions on Intelligent Transportation Systems*, 16(5):2786–2796, 2015.

[59] Rari Abousleiman and Osamah Rawashdeh. Energy consumption model of an electric vehicle. *2015 IEEE Transportation Electrification Conference and Expo, ITEC 2015*, (1):1–5, 2015.

[60] Juan Van Roy, Niels Leemput, Sven De Breucker, Frederik Geth, Peter Tant, and Johan Driesen. An Availability Analysis and Energy Consumption Model for a Flemish Fleet of Electric Vehicles. *European Electric Vehicle Congress EEVC*, pages 1–12, 2011.

[61] Jiang Bo Wang, Kai Liu, Toshiyuki Yamamoto, and Takayuki Morikawa. Improving Estimation Accuracy for Electric Vehicle Energy Consumption Considering the Effects of Ambient Temperature. *Energy Procedia*, 105:2904–2909, 2017.

[62] Xinkai Wu, David Freese, Alfredo Cabrera, and William A. Kitch. Electric vehicles' energy consumption measurement and estimation. *Transportation Research Part D: Transport and Environment*, 34:52–67, 2015.

[63] Cedric De Cauwer, Joeri Van Mierlo, and Thierry Coosemans. Energy consumption prediction for electric vehicles based on real-world data. *Energies*, 8(8):8573–8593, 2015.

[64] Jiquan Wang, Igo Besselink, and Henk Nijmeijer. Electric vehicle energy consumption modelling and prediction based on road information. *World Electric Vehicle Journal*, 7(3):447–458, 2015.

[65] Engin Ozatay. *Driving Profile Optimization for Everyday Driving*. PhD thesis, The Ohio State University, 2014.

[66] Meiqi Liu, Meng Wang, and Serge Hoogendoorn. Optimal Platoon Trajectory Planning Approach at Arterials. *Transportation Research Record*, 2019.

[67] Ganesh Mohan, Francis Assadian, and Stefano Longo. Comparative analysis of forward-facing models vs backward-facing models in powertrain component sizing. 2013.

[68] Tony Markel, Aaron Brooker, Terry Hendricks, Valerie Johnson, Kenneth Kelly, Bill Kramer, Michael OâKeefe, Sam Sprik, and Keith Wipke. Advisor: a systems analysis tool for advanced vehicle modeling. *Journal of power sources*, 110(2):255–266, 2002.

[69] Chiara Fiori, Kyoungho Ahn, and Hesham A. Rakha. Power-based electric vehicle energy consumption model: Model development and validation. *Applied Energy*, 168:257–268, 2016.

[70] Joel Andersson. *A General-Purpose Software Framework for Dynamic Optimization*. PhD thesis, Arenberg Doctoral School, KU Leuven, Department of Electrical Engineering (ESAT/SCD) and Optimization in Engineering Center, Kasteelpark Arenberg 10, 3001-Heverlee, Belgium, October 2013.

[71] Rajesh Rajamani. *Vehicle dynamics and control*. Springer Science & Business Media, 2011.

[72] Zongxuan Sun and Guoming G Zhu. *Design and control of automotive propulsion systems*. CRC press, 2014.

[73] Bingzhan Zhang, Chris Chunting Mi, and Mengyang Zhang. Charge-depleting control strategies and fuel optimization of blended-mode plug-in hybrid electric vehicles. *IEEE Transactions on Vehicular Technology*, 60(4):1516–1525, 2011.

[74] James Larminie and John Lowry. *Electric vehicle technology explained*. John Wiley & Sons, 2012.

[75] Student Competitions Team MathWorks. MATLAB and Simulink Racing Lounge: Vehicle Modelling, 2019. MathWorks.

[76] Martin Treiber, Ansgar Hennecke, and Dirk Helbing. Congested traffic states in empirical observations and microscopic simulations. *Physical review E*, 62(2):1805, 2000.

[77] Allego. The World of Electric Charging Costs, 2019. Allego B.V.

[78] BW Bader. Constrained and unconstrained optimization. 2009.

[79] Wouter J Schakel, Bart Van Arem, and Bart D Netten. Effects of cooperative adaptive cruise control on traffic flow stability. In *13th International IEEE Conference on Intelligent Transportation Systems*, pages 759–764. IEEE, 2010.

Appendices

Appendix A.

Virginia Tech Comprehensive Power Based EV Energy consumption Model (VT-CPEM) parameters

Table A.1. – Parameters and coefficients for energy consumption model

Notation	Parameter/coefficient	Value	Unit
m	Mass of the vehicle	1595	kg
g	Gravitational acceleration	9.8066	m/s^2
θ	Road grade	0	deg
C_r	Rolling resistance parameter for road surface	1.75	-
c_1	Rolling resistance parameter for road condition	0.0328	-
c_2	Rolling resistance parameter for vehicle tyre type	4.575	-
ρ_{air}	Air mass density	1.2256	kg/m^3
A_f	Frontal area of the vehicle	2.3316	m^2
C_D	Aerodynamic drag coefficient	0.28	-
η_d	Driveline efficiency	92	%
η_m	Electric motor efficiency	91	%
η_{rb}	Regenerative braking efficiency	-	%
η_b	Battery efficiency	90	%
$C_{Battery}$	Battery capacity	24	kWh
$P_{Auxiliary}$	Auxiliary power	700	W

Appendix B.

Sequential Quadratic Programming

Sequential Quadratic Programming (SQP) is a constrained optimization algorithm. The objective function $f(x)$ may be any smooth nonlinear function (atleast twice continuously differentiable). The constraints $\mathbf{h(x)}$ and $\mathbf{g(x)}$ are any nonlinear functions [78]. SQP's concept is to approximate the given NLP at each iteration x_k with a local model that is represented by a simpler Quadratic Programming (QP) sub problem. A general optimization problem in the negative null form is given by:

$$\begin{aligned} \min_{\mathbf{x}} & f(\mathbf{x}) \\ \text{s.t.} & \mathbf{g}(\mathbf{x}) \leq \mathbf{0} \\ & \mathbf{h}(\mathbf{x}) = \mathbf{0} \end{aligned} \tag{B.1}$$

$$\tag{B.2}$$

B.0.1. KKT Conditions

KKT conditions are necessary conditions for local constrained minima. Combining the Lagrange conditions for equality and inequality constraints yields KKT conditions for the general problem:

$$\begin{aligned} \frac{\partial L}{\partial \mathbf{x}} = \frac{\partial f}{\partial \mathbf{x}} + \sum \mu_i \frac{\partial g_i}{\partial \mathbf{x}} + \sum \lambda_i \frac{\partial h_i}{\partial \mathbf{x}} = 0 \\ \mu_i g_i(x) = 0 \forall i \\ \mathbf{g} \leq 0 \qquad \mathbf{h} = 0 \\ \mu \geq 0 \qquad \lambda \neq 0 \end{aligned} \tag{B.3}$$

The first KKT condition can be solved using Newton Method. For simplification we use a combined Lagrangian multiplier $\lambda = [\mu\lambda]^T$ and constraint $\mathbf{h} = [\mathbf{gh}]^T$. Inequality constrains can be made equal using slack variables and this doesn't alter the nature of the problem/-solution. Newton formulation is given by:

$$\begin{bmatrix} \frac{\partial^2 L}{\partial \mathbf{x}^2} & \frac{\partial^2 L}{\partial \mathbf{x} \partial \lambda} \\ \frac{\partial^2 L}{\partial \mathbf{x} \partial \lambda} & \frac{\partial^2 L}{\partial \lambda^2} \end{bmatrix} \begin{Bmatrix} \Delta \mathbf{x} \\ \Delta \lambda \end{Bmatrix} = - \begin{Bmatrix} \frac{\partial L}{\partial \mathbf{x}} \\ \frac{\partial L}{\partial \lambda} \end{Bmatrix} \tag{B.4}$$

Substituting for L and from equation B.4, we obtain

$$\begin{bmatrix} \mathbf{W} & \mathbf{A}^T \\ \mathbf{A} & \mathbf{0} \end{bmatrix} \begin{Bmatrix} \Delta\mathbf{x} \\ \Delta\lambda \end{Bmatrix} = \begin{Bmatrix} -\nabla f - \mathbf{A}^T\lambda \\ -\mathbf{h} \end{Bmatrix} \tag{B.5}$$

Here $W = \frac{\partial^2 f}{\partial \mathbf{x}^2} + \lambda^T \frac{\partial^2 \mathbf{h}}{\partial \mathbf{x}^2}$ and $A = \frac{\partial \mathbf{h}}{\partial \mathbf{x}}$.
Substituting $\Delta\lambda k = \lambda k + 1 - \lambda_k$ in the above equation and rearranging we obtain

$$\begin{bmatrix} \mathbf{W} & \mathbf{A}^T \\ \mathbf{A} & \mathbf{0} \end{bmatrix} \begin{Bmatrix} \Delta\mathbf{x} \\ \lambda_{k+1} \end{Bmatrix} = \begin{Bmatrix} -\nabla f \\ -\mathbf{h} \end{Bmatrix} \tag{B.6}$$

This matrix gives us two relations:

$$\mathbf{W}\Delta\mathbf{x} + \nabla f + \mathbf{A}^T\lambda_{k+1} = \mathbf{0} \tag{B.7}$$

$$\mathbf{A}\Delta\mathbf{x} + \mathbf{h} = \mathbf{0} \tag{B.8}$$

from above equations the modified quadratic sub problem can be formulated by multiplying with Δx and taking the whole transpose.

The solution to the KKT condition is the solution to the below quadratic subproblem:

$$\min_{\Delta\mathbf{x}} \frac{1}{2}\Delta\mathbf{x}^T\mathbf{W}\Delta\mathbf{x} + \nabla f^T\Delta\mathbf{x} \tag{B.9}$$

$$\text{s.t.} \mathbf{A}\Delta\mathbf{x} + \mathbf{h} = \mathbf{0} \tag{B.10}$$

This quadratic problem can be solved efficiently using quadratic programming. The solution to this problem is $\Delta\mathbf{x}$ which gives us the updated new design point $\mathbf{x}_{k+1}$

B.0.2. Algorithm Flow

The basic flow of the SQP algorithm is given below:

1. Choose an initial point $\mathbf{x}_0$ and lagrangian multiplier estimates λ_0.
2. Setup the Quadratic Programming sub problem as given in equation B.10.
3. Solve the QP subproblem to obtain $\Delta\mathbf{x}_k$ and λ_{k+1}
4. Update the design point $\mathbf{x}_{k+1} = \mathbf{x}_k + \Delta\mathbf{x}_k$
5. Check termination / convergence criteria. If satisfied stop else iterate again starting from 2.

For convergence Hessian must be positive definite. Computation of gradient information is necessary. Computation of hessian information can be performed if its calculation is efficient, this is called the exact method. If hessian evaluation is costly, then quazi-Newton approaches such as DFP and BFGS can be used to evaluate the hessian. In our problem the energy consumption model is twice differentiable and the constraints are atleast once differentiable. Therefore, hessian and gradient informations can be computed.

Appendix C.

Intelligent Driver Model

The Intelligent Driver Model (IDM) is used to represent ACC vehicles [76]. It is one of the models that attempted to capture human driving behaviour in a car following model. The distinctive feature of this model is the nonlinear response to speed differences []. The IDM acceleration $\dot{v}(t)$ is given by

$$\dot{v}(s, v, \Delta v) = a \left[1 - \left(\frac{v}{v_0} \right)^4 - \left(\frac{s^*(v, \Delta v)}{s} \right)^2 \right] \tag{C.1}$$

The above equation can be divided into two parts. The first part acceleration term $\dot{v}_{free}(v) = a[1 - (v/v_0)^4]$ and second term $\dot{v}_{brake}(s, v, \Delta v) = -a(s^*/s)^2$ as braking term. The acceleration term represents the behaviour of the vehicle when driving on a road without congestion. The braking term denotes the acceleration behaviour of the vehicle when approaching the leading vehicle (i.e) the following vehicle must decelerate to avoid rear end collision [79]. In the equation C.1, the term s^* represents the dynamic desired headway as a function of speed and speed differences written as follows

$$s^*(v, \Delta v) = s_0 + vT + \frac{v\Delta v}{2\sqrt{ab}} \tag{C.2}$$

where,
a is the comfortable acceleration
v is the current speed
v_0 is the desired speed
s_0 is the minimum headway at standstill
T is the desired time headway
Δv is the speed difference with the leader
s is the current distance headway
b is the comfortable deceleration.

Table C.1, shows the parameters and coefficients of IDM

Table C.1. – Parameters and coefficients of IDM

Notation	Parameters/coefficients	Value	Units
a	Comfortable acceleration	2	m/s^2
b	Comfortable deceleration	5	m/s^2
v_0	Desired speed	15	m/s
T	Time headway	2	s
s_0	Minimum gap	2	m